

Reliability and Economic Analysis of a Microgrid System:
A Case Study of Ifite Community, Nigeria

Author: Franklin Chukwuebuka Nkado

Supervisor: Dr Ramon Zamora

A thesis submitted to
Auckland University of Technology
In fulfilment of the requirements for the degree of
Master of Engineering (MEng)

2021

School of Engineering
School of Engineering, Computer and Mathematical Sciences

Abstract

With frequent power outages in Nigeria's Ifite community, which relies only on a diesel generator, solar energy has been recognized as a viable alternative to meet the community's growing energy demand. However, due to photovoltaics' (PV) high initial cost of installation and intermittent nature, PV systems are not widely used in most Nigerian communities. Therefore, this thesis studies the feasibility of incorporating a Photovoltaic-Battery Energy Storage (PV-BES) into the existing Diesel Generator (DG) system to minimize the community's complete reliance on conventional energy while improving the microgrid's reliability. The study also minimizes the Levelized Cost of Energy (LCOE), Net Present Cost (NPC) and improve the reliability of the proposed microgrid system, which in turn reduces the outage hours and Cost of Load Loss (CLL).

The research aims to determine how integrating the PV-BES system to the existing DG significantly affect the reliability and economics of the community's DG microgrid system. The objective was achieved by utilizing the probability concept in MATLAB to obtain the reliability performance indicators such as the Loss of Load Probability (LOLP), Loss of Load Expectation (LOLE), Expected Energy not Served (EENS). Furthermore, the economic impacts of integrating PV-BES in the existing DG microgrid system were also investigated using MATLAB's `fmincon` optimization tool. Six scenarios with the same load profile, site irradiation, and diesel generator capacity were used to assess the proposed model's suitability. The proposed system was also modelled in HOMER to verify MATLAB's `fmincon` optimization tool's result and show the hourly variation of load demand and the generating units in the six scenarios. Additionally, factors such as the PV price, derating factor and azimuth angle effect on the PV energy production were utilized to study their impacts on the cost and operation of the proposed microgrid system. The results show that scenario six provides the optimum solution for the proposed PV-DG-BES with an LCOE of 0.209 \$/kWh, total NPC of \$614,191 and Initial capital cost of \$192,118. The proposed system also improved reliability indices; the LOLP reduced from 2.6 to 0, the LOLE decreased from 84 hr/year to 0 hr/year, the CLL declined from 8,500 \$/year to 0 \$/year and the EENS from 5,800 kWh/year to 0 kWh/year. To conclude, the analysis results show that scenario six is feasible regardless of the high initial capital cost.

Acknowledgements

First and foremost, I am grateful to God for enabling me to complete this research. Second, I would like to express my gratitude to the Ministry of Foreign Affairs and Trade (MFAT) of New Zealand for funding this research. The scholarship officers at AUT, Sacha Pointon, Petrina Hibben, George Kimani, Sandelyn Agnes Su Kuan Lua, Prerna Taneja and the rest of the scholarship staff deserve special thanks for their exceptional support and guidance.

In addition, I cannot thank my supervisor, Dr Ramon Zamora, enough for his assistance and guidance in completing my degree. Without his help, completing this laborious task would have been impossible. I would also like to thank my research group members (Nicholas Mukisa, Xin Lin, Asaad Muhammad, Ifedayo Oladeji, Peter Makolo, Charles Ofori, Guannan Xu and Arpana Korshapati) for their questions, suggestions and assistance during research group meetings. Finally, I want to thank my parents and siblings for their prayers and moral support throughout my academic career.

List of Abbreviation and Symbols

COE	Cost of Energy
CRF	Capital Recovery Factor
CLL	Cost of Load Loss
DOA	Days of Autonomy
DOD	Depth of Discharge
NPC	Net Present Cost
NPV	Net Present Value
PV	Photovoltaic
HOMER	Hybrid Optimisation of Multiple Energy Resources
LF	Load Following
EENS	Expected Energy not Served
LOLP	Loss of Load Probability
LOLE	Loss of Load Expectation
AFC	Annual Fuel Cost
ASC	Annual System Cost
BES	Battery Energy Storage
DG	Diesel Generator
LPT	Load Probability Table
FOR	Forced Outage Rate
COPT	Capacity Outage Probability Table
LDC	Load Duration Curve
RI	Reliability Index
$P(C_i)$	Probability of the state i
$P(L_i > C_i)$	Duration of loss of capacity in present
L_i	Expected Load Demand
C_i	Generation Capacity
P_k	Individual Probability of Capacity in an Outage
T_k	Number of days lost due to Power Outage
L_e	Value of the Lost Load

C_{afuel}	Annual Fuel Cost
C_{amain}	Annual Maintenance Cost
C_B	Battery Bank Capacity
V_B	Battery's Nominal Voltage
N_{BT}	Total Number of Batteries
N_{BS}	Number of Batteries connected in Series
N_{BP}	Number of Batteries connected in Parallel
η_{gen}	Diesel Generator Efficiency
α_p	Temperature Coefficient of Power
P_{gen}^{min}	Generator minimum Power Output
P_{gen}^{max}	Generator maximum Power Output
P_{PV}^{min}	PV maximum Power Output
P_{PV}^{max}	PV maximum Power Output
P_{Bess}^{min}	Battery minimum Power Output
P_{Bess}^{max}	Battery maximum Power Output

Table of Contents

Abstract.....	ii
Acknowledgements.....	iii
List of Abbreviation and Symbols	iv
List of Figures	viii
List of Tables	ix
Attestation of Authorship	x
Chapter 1 Introduction	1
1.0 Background	1
1.1 Problem Description	4
1.2 Rationale and Significance of the Study.....	5
1.3 Research Questions and Objectives.....	6
1.4 Contribution to the knowledge.....	6
1.5 Thesis Structure	7
Chapter 2 Literature Review	8
2.0 Overview	8
2.1 Reliability and Economic Evaluation of a Microgrid Power System	8
2.2 Review of Analytical Methods for Reliability Analysis	12
2.3 Other Methods of Reliability and Economic Analysis Techniques.....	13
2.4 Reliability Indices for Power Systems	15
2.5 The Capacity Outage Table (COT)	16
2.6 The Load Duration Curve (LDC).....	17
2.7 Economic Feasibility of a Microgrid System	18
2.8 Summary	19
Chapter 3 Methodology.....	20
3.0 Overview	20
3.1 Data Collection Method	20
3.1.1 System Load Profile.....	20
3.1.2 Solar Resource Data	21
3.1.3 Estimation of Load	23
3.2 Analytical Design Calculation	26
3.2.1 Solar PV System.....	26
3.2.2 Inverter Selection.....	27
3.2.3 Battery Bank Sizing.....	28
3.2.4 Diesel Generator Sizing	30

3.3	Simulation and Analysis using HOMER Pro Software	31
3.3.1	Solar PV Module.....	32
3.3.2	Sizing of Inverter	33
3.3.3	Battery Sizing	33
3.3.4	Diesel Generator	34
3.4	MATLAB Software Analysis	34
3.4.1	Problem Formulation	34
3.5	Constraint functions.....	36
3.5.1	Constraint on power balance.....	36
3.5.2	Constraints on output power.....	36
3.6	Configuration of the case study	36
3.7	Proposed Microgrid Algorithm	38
3.8	Microgrid system's Reliability Indices	39
3.9	Summary	42
Chapter 4 Results and Findings.....		43
4.0	Overview	43
4.1	Configuration of Scenarios.....	43
4.1.1	Scenario 1.....	46
4.1.2	Scenario 2.....	47
4.1.3	Scenario 3.....	49
4.1.4	Scenario 4.....	51
4.1.5	Scenario 5.....	52
4.1.6	Scenario 6.....	53
4.2	Sensitivity Analysis	54
4.2.1	Effect of PV price on LCOE	54
4.2.2	Azimuth Angle Effect on the PV Energy Production	55
4.2.3	PV Systems Performance Based on Derating Factor	56
4.3	Summary	58
Chapter 5 Conclusion, Limitation and Future Work		59
5.0	Conclusion.....	59
5.1	Limitation	60
5.2	Future work.....	60
Apendices.....		66

List of Figures

Figure 3.1: Estimated load profile for Ifite community	20
Figure 3.2: The proposed microgrid system of this study.....	21
Figure 3.3: Map of Anambra State showing the location of the study area [7].	22
Figure 3.4: Solar resource data for the study area on a monthly average	23
Figure 3.5: Load demand curve and baseload Profile.....	25
Figure 3.6: Capacities of the proposed microgrid components.....	31
Figure 3.7: HOMER Schematic for the proposed Microgrid	32
Figure 3.8: Flowchart for the LOLP calculation methodology.....	41
Figure 3.9: Research Methodology Flow chart	42
Figure 4. 1: Loss of Load Probability Results for the Scenarios.....	44
Figure 4.2: Loss of Load Expectation Results for the Scenarios.....	45
Figure 4.3: Expected Energy Not Served Results for the Scenarios.....	45
Figure 4.4: Cost of Load Loss Results for the Scenarios.....	46
Figure 4.5: Variation of power from DG and load demand and for Scenario 1	47
Figure 4.6a: Variation of power from PV-DG and load demand for scenario 2.....	48
Figure 4.6b: Aggregate power from PV-DG and load demand for scenario 2	48
Figure 4.7a: Variation of power from PV-DG-BES and load demand for scenario 3.....	50
Figure 4.7b: Aggregate power from PV-DG-BES and load demand for scenario 3.....	50
Figure 4.8a: Variation of power from PV-DG-BES and load demand for scenario 4.....	51
Figure 4.8b: Aggregate power from PV-DG-BES and load demand for scenario 4.....	50
Figure 4.9a: Variation of power from PV-DG-BES and load demand for scenario 5.....	52
Figure 4.9b: Aggregate power from PV-DG-BES and load demand for scenario 5.....	52
Figure 4.10a: Variation of power from PV-DG-BES and load demand for scenario 6.....	53
Figure 4.10b: Aggregate power from PV-DG-BES and load demand for scenario 6.....	53
Figure 4.11: Solar PV price effect on the LCOE of the PV-DG-Battery System	55
Figure 4.12: PV generated energy of Azimuth angle for 0° and 90°, 180° and 270°	56
Figure 4.13: Techno-Economic Effect of the three Derating Factors.....	57

List of Tables

Table 3.1: Total daily energy demand of all households in Ifite community.....	24
Table 3.2: The total daily energy demand of all households in Ifite community	25
Table 3.3: The array tilt angle and the design current.....	26
Table 3.4: The PV module requirement calculations.....	27
Table 3.5: The technical specification for the selected inverter.....	28
Table 3.6: Battery Specification	29
Table 3.7: Series and Parallel Battery Specifications	30
Table 3.8: System Battery Capacity	30
Table 3.9: The proposed Microgrid System's technical and financial parameters.....	31
Table 3.10: PV Module specification.....	33
Table 3.11: Battery Specification	34
Table 3.12: The microgrid system's technical and cost parameters [31, 66]	38
Table 3.13: Configuration of Scenarios	39
Table 3.14: COPT for diesel generator	40
Table 3.15: COPT for PV	40
Table 3.16: COPT for the Battery	40
Table 3.17: COPT of all the Units	40

Attestation of Authorship

I hereby declare that this submission is my own work and that, to the best of my knowledge and belief, it contains no material previously published or written by another person (except where explicitly defined in the acknowledgements), nor material which to a substantial extent has been submitted for the award of any other degree or diploma of a university or other institution of higher learning.

Signed

Franklin Nkado

.....

Date

16/07/2021

.....

Chapter 1 Introduction

1.0 Background

The world's population is rapidly increasing, which has resulted in a rise in energy consumption. In developing countries, the primary energy source is conventional energy sources (coal, natural gas, and oil). The high energy demand from conventional energy sources results in environmental problems such as carbon dioxide (CO₂) and greenhouse gas (GHG) emission [1]. An alternative energy source with the following characteristics, namely sustainable, efficient, and environmentally friendly, energy source is required to meet the increasing energy demand. The alternative energy sources can be installed as either a standalone or integrated system with conventional energy sources.

Due to its location in Sub-Saharan Africa (Latitude 9.0820°N and Longitude 8.6753° E), Nigeria has an enormous amount of available solar energy [2]. Nigeria receives an average sunshine duration of 12 hrs/day, where the solar radiation received in each respective part of the country are as follows: 22.88MJ/m²/day in the northern part, 18.29MJ/m²/day in the central part, and 17.08MJ/m²/day in the southern part [3]. The high solar radiation makes it a good location for photovoltaic (PV) system adoption.

However, one of Nigeria's biggest problems is how to balance the energy generated to meet the ever-growing energy demand. The electrification rate is around 55% in urban and 36% in rural areas [4]. Individuals and business owners have resorted to generating their electricity using gasoline and diesel generator sets because of the electricity generation's inadequacy and the unreliability of the transmission and distribution systems [5]. Nigeria has seven generation companies, known as GENCOs, responsible for power generation; and eleven distribution companies, known as DISCOs, responsible for distributing energy to end-users [6]. However, these DISCOs still experience difficulties in meeting the constant rise in energy demands from the end-users.

The Ngozi Okonjo-Iweala (NOI Polls) survey in 2013 shows that about 80% of Nigerians use alternative electricity supply sources, such as gasoline and diesel generator sets [4]. Nigeria is a major importer of generator sets in Africa, and there is a total of about 60 million diesel

generators in Nigeria. According to the Energy Commission of Nigeria (ECN), the private decentralized diesel generator's total capacity is about 2600 gigawatts (GW) [4]. The increase in diesel and gas generators use has negative economic and environmental consequences, such as noise and air pollution. Consequently, this makes Nigeria become the most producer of greenhouse gases (GHGs) in Africa. The Niger delta area in the southern part of Nigeria releases about 46 billion KW/year of heat into the air [7]. In addition, the country's economy is also affected by the importation of refined petroleum products and generating sets.

Nigeria developed an electrification plan which aims to extend electricity to rural communities. The program targets to increase the electrification percentage to 75% by 2020, 90% access to electricity by 2030 and 100% electrification by 2040 through renewable energy deployment. The program is proposed to extend electricity to an additional 1.1 million households yearly between 2015-2020 and 513,000 households between 2020 to 2040 [4]. Renewable energy technologies such as wind, solar, geothermal and biomass are becoming increasingly attractive because they are environmentally friendly [1]. Renewable energy is expected to become the fastest-growing global energy source, with an average consumption increase of 2.3% per annum between 2015 and 2040 [8]. Research projects are still ongoing in cost-effective ways to harness these clean and sustainable energy resources such as wind, solar, geothermal and biomass.

Nigeria has several renewable energy resources (RERs) which have not yet been fully explored, such as solar, geothermal, biomass and wind. Regardless of the abundant renewable energy resources present, Nigeria only generates around 1600 MW out of the 6000 MW installed electricity generating capacity, mainly because of the unreliability of the electricity generation systems [9]. Among the renewable resources found in Nigeria, solar energy resource is mostly preferred due to its abundance. Nigeria's total land area of $924 \times 10^3 \text{ km}^2$ receives about $1.804 \times 10^{15} \text{ kWh}$ of solar irradiation which irradiation, approximately $5.535 \text{ kWh/m}^2/\text{day}$. Approximately 3.7% of the country's acreage is required to harvest solar energy, to generate power equal to Nigeria's existing capacity [7]. Nigeria has proposed adopting and deploying renewable energy technology to solve fossil fuels' over dependency [4].

Though renewable energy is becoming increasingly attractive, renewable energy resources' intermittency is amongst the problems facing renewable energy technology. This is because most renewable resources depend on climatic influences such as solar irradiation, wind speed and ambient temperature. Many research projects have proposed using more than one renewable energy resources combined with diesel generator(s). Hence, the strength of the renewable energy resources can be effectively utilized to compensate for the diesel generator's weakness vice-versa [10]. The irregularity of the electricity produced from renewable energy generators such as photovoltaic (PV) has necessitated using a backup Energy Storage System (ESS) with renewable technology. ESS stabilizes the fluctuating energy produced by renewable energy generators and makes them as stable as conventional systems [10, 11]. Among the available energy storage systems, chemical batteries are mostly used, particularly lead-acid battery because of their availability and low cost [12].

A photovoltaic (PV) system is a type of renewable energy system that uses sunlight to generate electricity. It comprises solar cells arranged in series to form a PV module, and these modules absorb and convert sunlight into electricity. When designing the PV system, it is crucial to calculate the number of modules required to be connected in series or parallel to generate the desired energy level [3]. An arrangement of several interfacing components is required to convert, store and distribute electrical energy generated by a PV array. Such components include an inverter, a charge controller, and batteries for storing excess energy, depending on the system's functional requirement and type. For most community applications, lead-acid batteries are incorporated due to their low cost and availability [3].

The system may also require a charge controller to protect the battery from damage due to excessive charging and discharging. In some cases, the inverter may have a built-in charge controller that makes the need for an external charge controller unnecessary [3]. An inverter converts generated DC voltage to AC voltage in satisfying AC load. A standalone PV microgrid system is mostly used for places with no access to electricity or places with unreliable power supply. This system is also an excellent alternative to provide power in emergencies or natural disasters such as earthquakes, typhoons and hurricanes. The block diagram of a typical standalone PV system is shown in Figure 1.1.

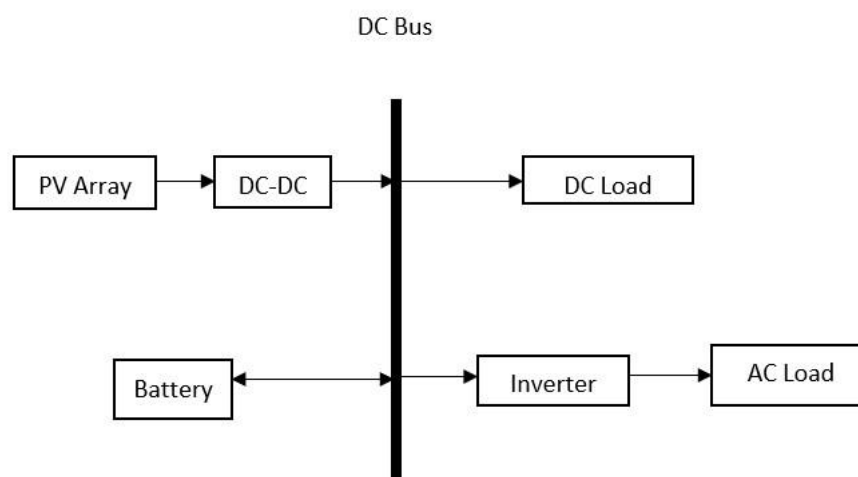


Figure 1.1: Standalone PV System

This thesis will study the feasibility of using a PV- generator with battery energy storage (BES) in a community of about 101 households and perform the system's economic and reliability assessment.

1.1 Problem Description

The growth in population has led to increasing electricity demand in Ifite community. In Anambra state, Nigeria, this community is located very far from the grid and has about 101 households [3]. This has forced the community to depend on a diesel generator, which runs continuously, making it expensive to operate due to the high fuel price and emits a large amount of greenhouse gas (GHG) into the environment. Also, due to the growing population of the area, the load demands have increased more than the capacity of the diesel generator resulting in frequent power outages.

Research on the cost and advantages of integrating solar PV in the microgrid is crucial for adopting and applying the PV technologies in the community so that the PV system's strength can be successfully used to supplement the community's traditional generating units' weaknesses and vice versa. Hence, there is a need to determine the effects of adding a new generating unit in the DG microgrid system.

However, the power system planning is required to determine the suitable design and components essential to meet the expansion of system load in the future with acceptable reliability and minimum operating and investment costs in the community; it is crucial to plan

the generation capacity with enough reserve to meet the load demand. The time duration for this study is 25 years considering the average panel lifetime of 25 years. Therefore, reliability studies are essential as part of power system planning to accurately determine the system's capacity to meet the load demand and effectively schedule repairs. The reliability of a component is its ability to perform a needed task in a specific environment, operational circumstances, and period [13]. Microgrid's function is primarily to supply the load demand at low-price and a satisfactory degree of reliability with environmental compliance [14]. As a result, it is crucial to plan for electricity to include integrating eco-friendly energy resources, guaranteeing that there would be enough energy reserve for future load expansion. Furthermore, the reliability assessment of microgrids is vital to limit the disruption of electrical services.

1.2 Rationale and Significance of the Study

The electricity demand increases in Nigeria because of the increasing population; the growing population requires more energy to meet its demand. The Nigerian Electricity Regulatory Commission (NERC) in 2016 signed a feed-in tariff into law to encourage the independent generation and reduce overloading the national grid. NERC also approved a generation capacity of 5,000 MW for an off-grid solar rooftop as part of the electrification strategy [3, 15]. Nigeria is progressing towards its 2040 vision, which aims to reduce the total dependence on oil to the bare minimum and focus on renewable resources. This plan will improve the economy of the country, as well as enhance environment cleanness.

Most individuals and communities in Nigeria have started adopting off-grid solar energy because it is more stable, reliable, and economical than the conventional grid. However, reliability assessment is necessary for the proposed microgrid's design to verify that the design meets the required reliability level defined by certain reliability indices. The reliability indices used in this thesis include Loss of Load Probability (LOLP), Expected Energy not Served (EENS) and Loss of Load Expectation (LOLE).

The important indices to determine the PV system's economic viability integrated into the power system are the Net Present Cost (NPC), Cost of Energy (COE), Cost of Load Loss (CLL), and Annual System Cost (ASC). These economic indices are used to determine the best feasible combination of the PV-BES when incorporated in the existing power grid. When

several options are being considered among many power generating units' combinations, the one with the lowest ASC, COE and NPC will be the most cost-effective alternative.

1.3 Research Questions and Objectives

The following research question was developed from the problem statement and discussion above:

How would integrating the PV-BES system to the existing DG significantly affect the reliability and economics of the community's DG microgrid system in 25 years?

The following sub-questions were formed from the research question to provide more detailed answers:

- 1) How would integrating a PV-BES system to the community's DG microgrid make the system more economical than using only DG?
- 2) How would integrating a PV-BES system to the community's DG microgrid make the system more reliable than using only DG?

To address the research question and its sub-questions, the following study objectives were defined:

- 1) To show the proposed microgrid's effect on the Cost of Energy (COE) by increasing the PV-BES system penetration level.
- 2) To show the proposed microgrid's effect on the reliability by increasing the PV-BES penetration level.
- 3) To test the suitability of different PV-BES system penetration level on various scenarios with the existing system.

1.4 Contribution to the knowledge

Reliability theory is used widely for power system reliability analysis [14, 16-19]. Conducting a reliability analysis for lower-level power system (microgrids) has not been common in literature. This research is the first of its kind in Nigeria. Therefore, this thesis will contribute to the advancing of knowledge in the following ways by:

- Providing an approach to evaluate the cost of energy (COE) before and after integrating a PV-BES to an existing DG microgrid system.

- Providing a method to show various PV-BES integration level's effect on the reliability of the existing DG microgrid system.

1.5 Thesis Structure

This thesis has five chapters, which are ordered as follows:

- Chapter 1 gives a background overview, problem description, rationale & significant of the study, the research objectives and questions and contribution to the knowledge.
- Chapter 2 shows an overview of microgrid reliability; it discusses various microgrid analysis methods. It also details the probabilistic concept of reliability, reliability indices and the economic feasibility of a microgrid system.
- Chapter 3 describes the methodology of this thesis; It focuses on designing and modelling the proposed microgrid system; it details PV-BES system analytical design and the use of HOMER software for the simulation and performance analysis of the proposed microgrid system. It also shows the fmincon optimisation method for economic and reliability analysis.
- Chapter 4 compares and discusses the outcomes of several scenarios with and without a PV system to demonstrate the impact of including a PV-BES system in the DG microgrid system.
- Chapter 5 summarises the study's findings, verifies that the research questions have been answered, and discusses future work.

Chapter 2 Literature Review

2.0 Overview

This chapter will summarise microgrid power system reliability and economic analysis and the various research and methods used in power system reliability analysis. Then, the capacity outage table and the load duration curve will be presented. Finally, the chapter will be summarized.

2.1 Reliability and Economic Evaluation of a Microgrid Power System

The ability of a power system to fulfil consumers' load demand at all times is referred to as reliability time [20]. A reliable power system is typically configured to provide enough power to satisfy load demand while requiring minimal investment cost and operating cost. A microgrid can function as a standalone or grid-connected system depending on the economic, reliability and environmental benefits that utilities gain by utilizing the system. As a result, performing an economic and reliability assessment of a microgrid system at the design stage is crucial.

In a power system, reliability studies are used by the utilities to evaluate the effects of adding or removing generators, transformers and lines. The performance indicators used to assess the power systems reliability at the generation level are Loss of Load Probability (LOLP), Loss of Load Expectation (LOLE), Expected Energy not Served (EENS), Cost of Load Loss (COLL). In addition, evaluating a power system reliability aims at system adequacy and security [21].

System Adequacy is the availability of adequate power system facilities to meet the load demand. Hence, the generated energy is adequately delivered to the end user's load by the transmission and distribution systems. Therefore, power system adequacy is associated with the power system's static conditions and does not consider the system's handling of unexpected disturbances during operation. System adequacy is best analyzed through power flow simulation studies [21].

System Security is the power system's ability to successfully handle unexpected disturbances during operation and still maintain a steady power balance [22]. Hence, system security relates to the power system's dynamic response to disturbances during operation.

The entire power system's reliability is complex to evaluate due to its size and the number of components in the system, which has different functions and objectives. Hence, reliability studies are classified into three parts known as Hierarchical levels HL: HL I (generation), HL II (transmission), and HL III (distribution) [23], as shown in Figure 2.1.

Hierarchical level I (HL I - generation) refers to the generation system facility capacity. At this level, a reliability evaluation is performed to determine if the total generation capacity will meet the expected system demand. The major indices used to measure the reliability level at HL I are the Loss of Load Probability (LOLP), Loss of Load Expectation (LOLE) and Expected Energy not Served (EENS) [24].

Hierarchical level II (HL II – generation + transmission) describes the generation facilities and transmission equipment's (transformers and lines) capacity to meet the load energy demand. The main indices considered here are Failure Duration (FD) and Failure Frequency (FF) [24].

Hierarchical level III (HL III – generation + transmission + distribution) refers to the entire power systems (generation, transmission and distribution). The evaluation of the HL III can be very complex because the evaluation at this level involves the three hierarchical levels starting from the generating point to the end user's load point. Therefore, evaluation of the entire system is not performed concurrently. The distribution systems' (HL III) reliability is analyzed separately, with the transmission system's evaluation results (HL II) as the HL III input. The major reliability indices considered in (HL III) evaluation are Customer Average Interruption Duration Index (CAIDI), System Average Interruption Frequency Index (SAIFI) and System Average Interruption Duration Index (SAIDI) [24]. The HL I reliability evaluation is essential for the planning and designing the power system to avoid oversizing the system's components, which increases the cost and installation of the equipment. This thesis focuses on the hierarchical level I (HL I) reliability analysis.

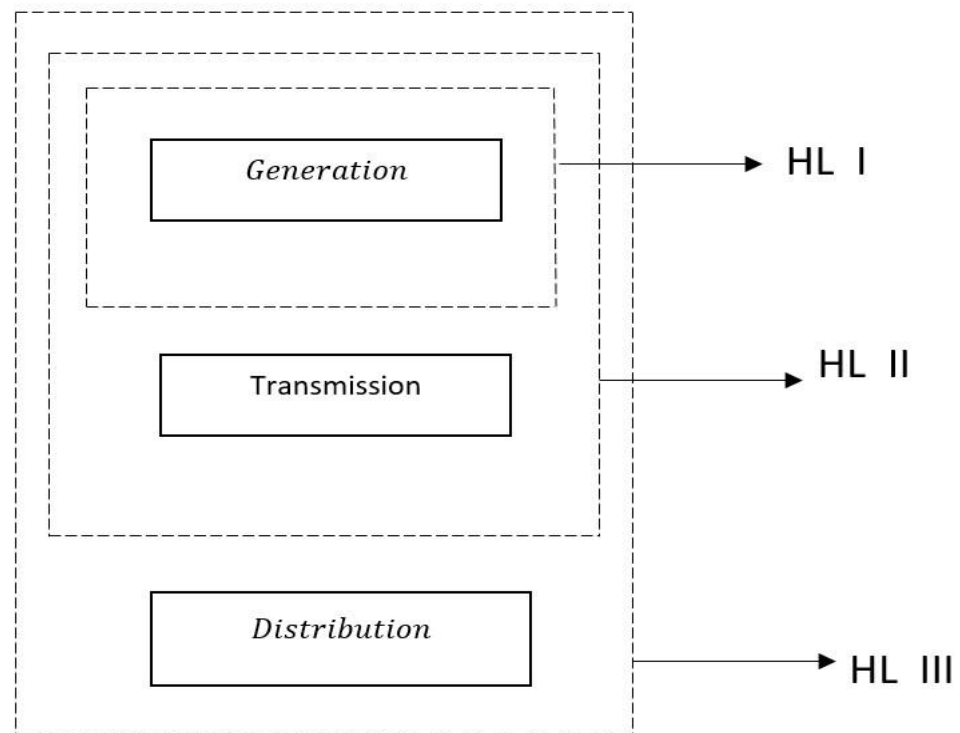


Figure 2.1: Power system's hierarchical level

Employing appropriate technique to analyze the system's adequacy is crucial during the microgrid's systems planning. Different methods of generation system reliability evaluation have been presented in [25, 26]. The deterministic and probabilistic methods are mostly used in generation system reliability analysis [27]. The deterministic approach uses mainly the thumb rule method, such as determining the capacity reserve or the (N-1). The N-1 criteria do not respond to component failures, while the probabilistic method considers stochastic system behaviour [28]. The probabilistic approach can use either the analytical or Monte Carlo simulation methods (MCSM), as shown in Figure 2.2 [29].

The analytical method represents the system model mathematically, while the MCSM involves more resources and computational time. MCSM consists of analyzing the system's random behaviour by simulating the components' physical characteristics. Also, a more complex component model, including component aging effect, failure rate, and shading effects of the power systems' components, utilizes the MCSM. However, MCSM has a high computational time [29].

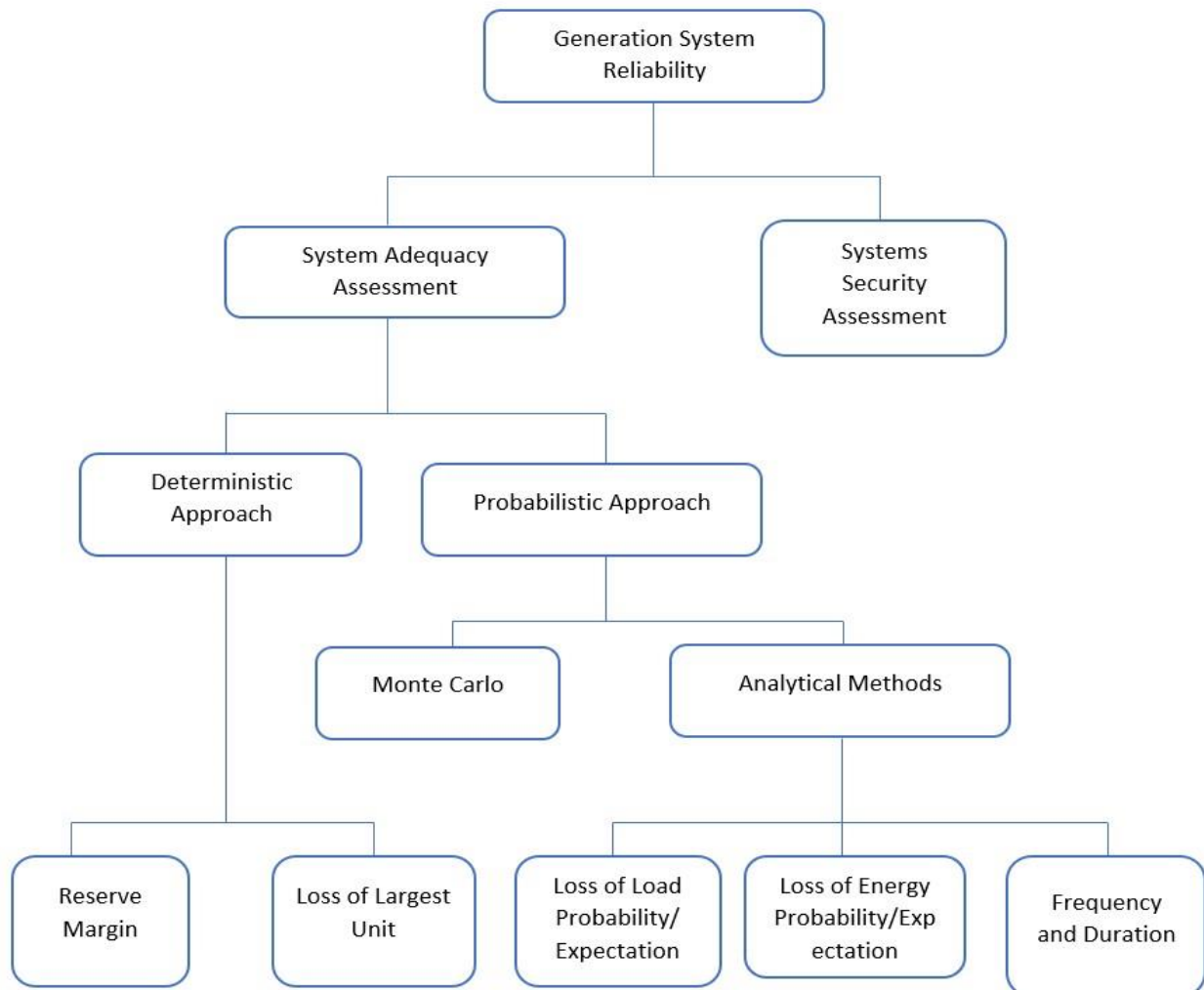


Figure 2.2: Generation system reliability assessment classification [30]

Therefore, the `fmincon` optimization method is preferred in this thesis because it is a state of the art of optimization technique that handles large scale programming problems fast [31]. `fmincon` optimization utilizes the failure rate of components for reliability simulation analysis. Failure rates of components are an essential factor used when analyzing the system's random behaviour. Failure rates of components can be obtained from the component's accelerated life testing but are best determined from field data on the component's failure times. PV, battery and inverter manufacturers carry out accelerated life tests and collect data on their products' failure rate. Failure rates of components are also estimated with the model of component aging based on temperature, operating environment, voltage stress and other necessary factors [32, 33]. However, these data are not easily made available for public use. The failure rates used in this thesis were obtained from the literature [34, 35], which has the same degradation rate and operating environment as this thesis' case study.

The monte Carlo simulation methods are usually time-consuming due to the many calculations required to get accurate results [36]. Literature [27] analyzed a microgrid with various configurations, including photovoltaic (PV), micro gas turbine (MGT), wind turbine generator (WTG), and diesel generator (DG). Each supply's generation is modelled and compared to the IEEE RTS load model. The authors developed the WTG and PV generation models using the two-state reliability model and output control. To test reliability indices, these models were added to the Monte Carlo Simulation (MCS) process. The results obtained show that the first case study (optimal case study), consisting of ten 32-kW DG and five 60-kW MGT, has a Loss of Load Expectation (LOLE) of 0.176 day/year and a Loss of Load Frequency (LOLF) of 0.141 occurrences per year. The sixth case study (worst case study) consists of eight 32-DG, five 60-kW MGT, one 40-kW PV and two 20-kW WTG with an LOLE of 1.475 day/yr and a LOLF of 0.991 occ/yr. In addition, the authors concluded that the MGT is more cost-effective than the DG by comparing these two sources. However, they also specified that the PV and WTG systems are more unreliable in the study location than other renewable energy resources.

A Monte Carlo simulative technique to evaluate microgrids' reliability, including Diesel Generators (DGs) and Energy Storage System (ESS), was studied in [37]. The photovoltaic and wind power stochastic behaviour was first determined, followed by developing the combined DGs and ESS output models. The model was applied in the proposed Monte Carlo reliability evaluation algorithm. Finally, the authors verified the proposed technique's validity on the modified IEEE RBTS Bus 4 system containing two microgrids.

The reliability results show that DGs and ESS significantly impact the end user's power supply reliability within microgrids. The microgrid's failure rate and annual average disruption time of the load points decreased significantly.

2.2 Review of Analytical Methods for Reliability Analysis

The analytical methods are Less time-consuming than the Monte Carlo Simulation Technique. The statistical distribution of failure and repair rates are assumed in the analytical method. The Loss of Load Probability (LOLP) for a generation system was analyzed in [38] to determine the Force Outage Rate's (FOR) effect on the LOLP indices. The authors utilised the FOR values of 0.01, 0.02 and 0.05 on the power system, which comprises four generation companies with

six units. The Load Probability Table (LPT) was generated using the daily peak load for a year. The simulation results show that varying the power systems' component FORs affects the LOLP indices. For example, at 0.01 FOR, the LOLP indices was 5.043, while at 0.05 FOR, the LOLP indices increased to 7.52. However, the study did not consider other reliability indices such as the Loss of Load Expectation (LOLE), Expected Energy not Served (EENS) and Cost of Load Loss (CLL).

The study in [35] designed and analyzed a hybrid mini-grid system's technical and economic aspects for a typical Nigerian rural population, utilizing HOMER Pro software. The study has 2.5MWh/day residential load demand and 165kWh/day commercial load demand. HOMER's optimal solution included a 1,500kW solar PV system, 1,200 deep cycle batteries, and a 350kW diesel generator with operating costs of \$148,296 per year, \$0.396 per kWh Levelized Cost of Energy (LCOE), and a Net Present Cost (NPC) of \$4,909,206. The HOMER Pro software simulation results were validated using the Capacity Outage Probability Table (COPT) and the system's components' Forced Outage Rate (FOR). The study's value for Loss of Load Probability (LOLP), Loss of Load Expectation (LOLE), and Expected Load Loss (ELL) were calculated to be 5.76×10^{-8} , 5.0457×10^{-4} hrs./yr., and 0.025344 watt, respectively. The findings were compared to those of a related study in [34] that used a hybrid system design that included diesel generator, solar PV, wind turbines and energy storage facilities. The comparison results show that the study [34] has a lower LOLP value of 2.81×10^{-10} and LOLE of 2.46×10^{-6} hr/yr because of the wind turbine contained in the system. However, the study did not consider the degradation rate, the effect of PV price on the LCOE, derating factor effect on the PV energy production and the azimuth angle effect on the PV energy production.

2.3 Other Methods of Reliability and Economic Analysis Techniques

Several approaches for studying the effect of integrating renewable energy generators and Battery Energy Storage (BES) on a power system's efficiency and economic output have been suggested in studies [19, 39, 40]. The Particle Swarm Optimisation (PSO) approach was suggested in the literature [41] to reduce a PV-microgrid system's emission and operational costs. An energy management framework was proposed considering the load-following performance of dispatchable Diesel Generators (DGs). The proposed energy management approach and simulation findings for real-time application were assessed using a sample

microgrid. The authors in [31] used the MATLAB fmincon optimization method to investigate the economic effects of WTG, PV, and BES in a microgrid system. The research also used a probabilistic approach to assess the power system's reliability. The study's findings indicate that the use of renewable energy resources (RERs) will reduce the amount of service disruption and cost associated with a power outage.

The optimum operation of a PV system was determined using Hybrid Optimisation Model of Electric Renewable (HOMER) and System Advisor Model (SAM) [42-44] in Uganda [45] and India [44]. Furthermore, the HOMER pro software has been compared with other simulation tools such as SAM, Blue sol and Sunny design. HOMER pro software has shown to be better in determining the microgrid system's performance [46]. A hybrid renewable energy system with a PV, wind turbine, diesel generator and battery is proposed in the study [47] to provide electricity for Giri village in north-central Nigeria. The HOMER simulation tool was used for modelling and simulation of the system. The system's optimal configuration was determined based on the lowest NPC of \$1.01 and COE of \$0.110/kWh. Based on the sensitivity variables, which are solar radiation and diesel price, the diesel price was varied from \$0.7-\$0.8 per litre while the solar radiation also varies between 4.2 kW/m² /day and 5.9 kW/m² /day. The results reveal that the NPC and COE decrease with lower fuel prices and higher solar radiation values and increase with high fuel prices and lower Solar Radiation values.

The effect of PV degradation rate on the LCOE in Thailand was studied in the literature [48]. The study obtained the degradation rates of 73 PV modules of four different technologies: hetero-junction Si, multi c-Si, CIGS and micro-morph. The modules' degradation rates were obtained at a Thailand test site by generating 10kW electricity with the 73 modules. The LCOE was calculated based on the operational year, not on the 25 years warranty period and by assuming a fixed investment and annual operating cost for the PV system. The authors also assumed a fixed interest rate for all PV degradation rates for the analysis. The range of the LCOE obtained from the PV modules was between 4.1 to 14.0 baht/kWh, which is higher than current Thailand's residential rate of 3.8 baht/kWh. However, the authors noted that a 0.2%/year PV degradation rate or lower could reduce the PV system's LCOE to the current Thailand's residential electricity price.

2.4 Reliability Indices for Power Systems

Reliability indices may be used to evaluate the benefits of incorporating RERs into a microgrid system. The reliability indices are used by utilities to measure their networks' overall adequacy and forecast future power demand based on the reliability evaluation performance. RERs have a significant impact on load centres and the reliability of the power grid. The study of the impact of RERs on the power system has necessitated researchers and the utilities to use various methods to carry out a microgrid system's reliability evaluation. The most widely used indices for evaluating the reliability of generation systems are the Loss of Load Probability (LOLP), Loss of Load Expectation (LOLE), and Expected Energy Not Served (EENS) [31, 34, 35].

- **Loss of Load Probability (LOLP)**

LOLP is the possibility that the system's hourly demand or daily peak will exceed the available generating power in a given period. LOLP can be used to determine what additional capacity might be needed to meet the reliability targets. A standard industry target for the loss of load probability is not to exceed more than one day in ten years [35, 49].

The number of days in a year where the daily peak load exceeds the generation capacity is determined by taking the probability of generation capacity and multiplying it by the daily peak probability. The LOLP calculation can consider daily peak loads for each hour's load over a 24-hour day or a year. Consequently, depending on the desired outcome, the same system could have one or more LOLP values. Equation (2.1) shows the mathematical formula for calculating LOLP [38] [49].

$$LOLP = \sum_{i=1}^n P(C_i) \cdot P(L_i > C_i) \quad (2.1)$$

where $P(C_i)$ is the probability of a loss in capacity; L_i is the expected load demand; C_i is the generation capacity; $P(L_i > C_i)$ is the duration of the loss of capacity; n is the number of capacity outage state in excess of the reserve.

- Loss of Load Expectation (LOLE)

LOLE is the estimated duration (hours or days in a year) in which the available generation capacity would be insufficient to satisfy the consumers' power demand [1]. It is calculated by multiplying the probability of daily peak demand exceeding available capacity on each day by the number of days in a year. The LOLE is calculated by using Equation (2.2).

$$LOLE = \sum_{i=1}^n P_k \cdot t_k \quad (2.2)$$

where P_k is the individual probability of capacity in an outage; T_k is the number of days lost due to a power outage.

- Expected Energy Not Served (EENS)

EENS is a reliability index used to measure energy shortage when the demanded load exceeds the available generation capacity; it calculates the total energy not delivered to the load [35]. The EENS is calculated by using Equation (2.3)

$$EENS = \sum_{i=1}^n (L_i - C_i) \cdot P_i \times 8760 \text{ (kWh/yr.)} \quad (2.3)$$

where the load curtailment is expressed as $C_k = (L_i - C_i)$, L_i is the expected Load demand; C_i is the generation Capacity; and P_i is the probability of specific capacity outage.

- Cost of Load Loss (CLL)

The utility provider uses the CLL to monetize the cost of a power outage in a system. EENS' financial worth is calculated by multiplying it by the value of the lost load (L_e). The residential consumers' value of Lost load (L_e) in literature [50] ranges from 2 – 12 \$/kWh and 5 – 40 \$/kWh for residential and industrial applications, respectively. This study assumed the value of 1.5 \$/ kWh for the residential load loss value due to power outage. Equation (2.4) presents the formula used to estimate the power system's reliability value, focusing on the load loss cost (CLL) resulting from the power outage.

$$CLL = \sum_{i=1}^n (L_e \cdot EENS) \text{ (\$/yr)} \quad (2.4)$$

2.5 The Capacity Outage Table (COT)

The COT is used to compute the probability that the total generation capacity is unavailable due to forced outages exceeding a particular threshold [51]. The table's first column lists all

of the capacity states in ascending order of outage severity. The COT can be calculated using the binomial distribution of the system. The second column lists the corresponding probability of outages for a particular capacity state. With the aid of the load duration curve (LDC), the COT is used to calculate the LOLP. Also, the COT indicates the expected generation margin which is the difference between the available power generated and the load demand.

2.6 The Load Duration Curve (LDC)

The LDC shows the relationship between capacity utilization and the duration for which a load is served. It is a load curve in which the demand data is arranged in the order of descending magnitude. The LDC of Figure 2.3 is shown in Figure 2.4.

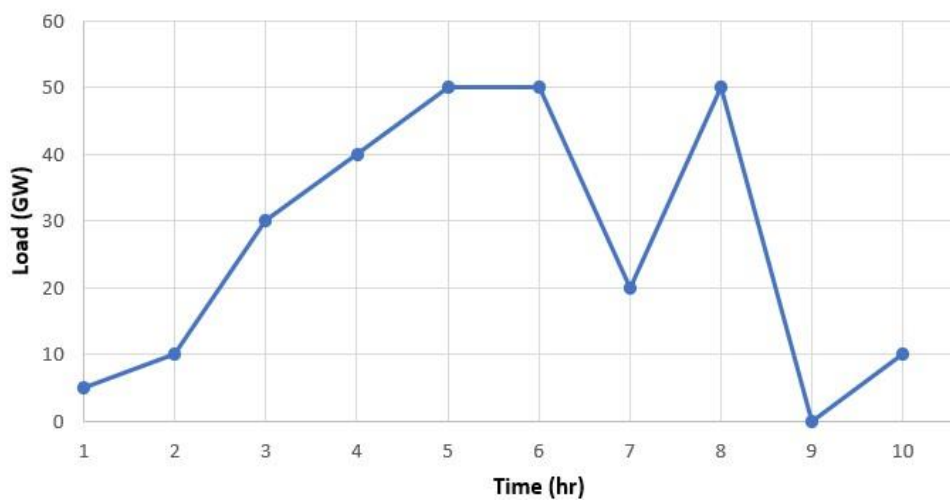


Figure 2.3: Example of a load curve

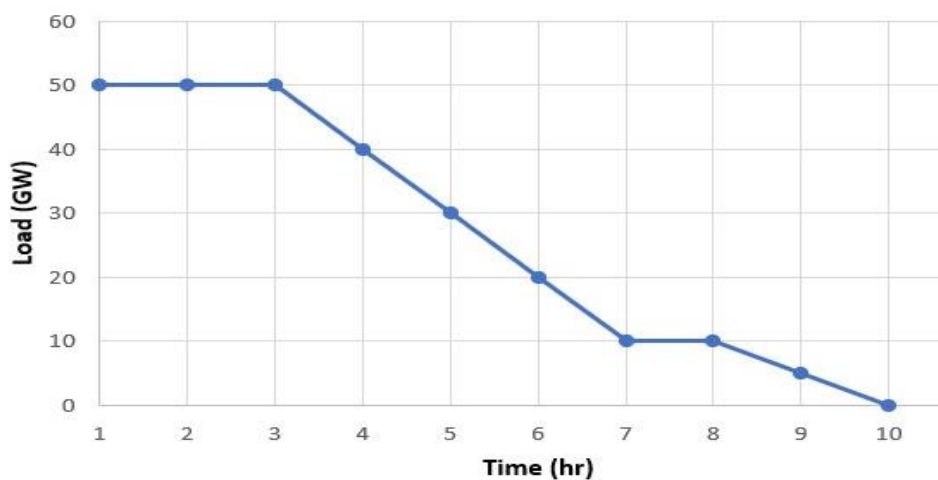


Figure 2.4: The load duration curve derived from Figure 2.3.

The LDC is used as a tool to illustrate the mix of various generation technologies serving load in the same power system [52]. For each capacity level of a COT, the percentage of time for each demand level is accrued from the LDC and subsequently used to calculate the LOLP of the power system under study.

2.7 Economic Feasibility of a Microgrid System

The significant criteria for determining a microgrid power system's economic feasibility are the Net Present Cost (NPC) or the Lifecycle Cost (LCC) and Levelized Cost of Energy (LCOE) [43, 45, 53, 54]. However, other indicators such as Annual System Cost (ASC), Internal Rate of Return (IRR), Net Present Value (NPV) and simple payback period (SPBP) are also used [43, 55, 56]. The NPC considers the average cost accrued during the microgrid's lifecycle, excluding costs incurred at disposal. The NPC values used in this study considered capital cost, annualised system cost, replacement cost and operation and maintenance cost [54].

The NPC of the microgrid system adds the system's components total cost such as the PV cost (C_{pv}), inverter cost (C_{inv}), battery cost (C_{batt}), battery replacement cost ($C_{batt\ repl}$), inverter replacement cost ($C_{inv\ repl}$), installation cost (C_{inst}) and the operation and maintenance cost ($C_{O\&M}$), of the system over a period in years. Equation (2.5) shows how NPC is calculated [54].

$$NPC = (C_{pv}) + (C_{inv}) + (C_{batt}) + (C_{batt, repl}) + (C_{inv repl}) + (C_{inst}) + (C_{O\&M}) \quad (2.5)$$

Levelized cost of energy (LCOE) measures the annual cost of producing electricity ($NPC_{1\ year}$) by dividing the ($NPC_{1\ year}$) by the useful energy generated from the renewable energy source (E_{RES}). Equations (2.6) and (2.7) are used to calculate the LCOE [54] while Equation (2.8) is used to determine the LCOE when considering the effect of PV's degradation on the LCOE.

$$LCOE = \frac{NPC_{1\ year}}{E_{PV}} \quad (2.6)$$

$$NPC_{1\ year} = \frac{NPC}{\frac{(1+i)^N}{i(1+i)^N}} \quad (2.7)$$

where i is the discount rate; N is the life span in years; and E_{PV} is the Energy generated by PV.

$$LCOE = \frac{\sum_{t=1}^n \left(\frac{I_t + M_t}{(1+i)^t} \right)}{\sum_{t=1}^n \left(\frac{E_{pv}(1-d)^t}{(1+i)^t} \right)} \quad (2.8)$$

where I_t is the investment cost; M_t is the maintenance cost; E_{pv} is total PV generated energy; i is the discount rate; d is the degradation rate; and n is the project lifetime in years.

- **Annualized Fuel Cost (AFC)**

The AFC is the fuel cost of operating the generator in a year which can be used to obtain the total fuel cost over system's lifespan. The annual fuel cost for a microgrid system consisting of DG is estimated using Equation (2.9).

$$AFC = C_{afuel} \sum_{i=1}^n [DG] \quad (2.9)$$

where C_{afuel} is the fuel cost for n th year; DG is the diesel generator being analysed.

2.8 Summary

The power system reliability assessment classification and theoretical analysis of various reliability & economic measurement approaches have been presented. Furthermore, the economic viability of a microgrid system, and a theoretical review of the power system reliability assessment classification were also presented.

From the reviewed literature, researchers have employed different techniques for the power system reliability analysis. However, to the best of the author's knowledge, none of these researchers used the reliability indicators, the annual cost of load failure, the effect of PV price on LCOE, azimuth angle effect on the PV energy production and the derating factor effect on PV simultaneously as the objective functions.

Chapter 3 Methodology

3.0 Overview

This chapter will start by discussing the data collection method adopted, then presenting the analytical method used to size the proposed microgrid components (PV, inverter, battery and diesel generator) and the components' technical specifications. Next, the chapter will show how HOMER software is used to simulate and verify the proposed system. Lastly, reliability and economic analysis utilizing fmincon optimisation in MATLAB will be presented.

3.1 Data Collection Method

3.1.1 System Load Profile

This study considered Ifite community in Anambra state, Nigeria, located at coordinates 6.604 °N and 6.951 °E. The community's daily load was estimated at 476.36 kWh based on the 2018 survey [3]. This study used the electricity demand data reported in study [3] because it best reflects Ifite community in terms of the daily usage of electrical appliances. Figure 3.1 shows the Ifite community load profile which was utilized to propose the microgrid system shown in Figure 3.2.

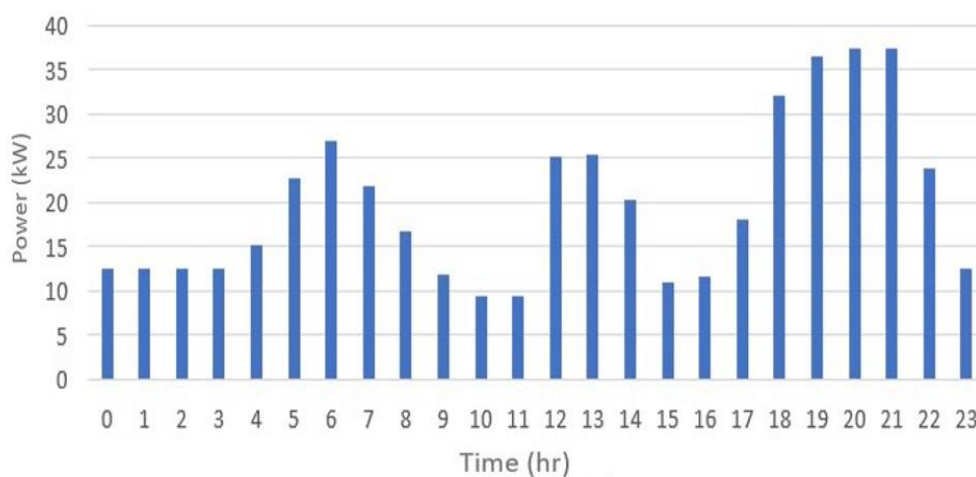


Figure 3.1: Estimated load profile for Ifite community

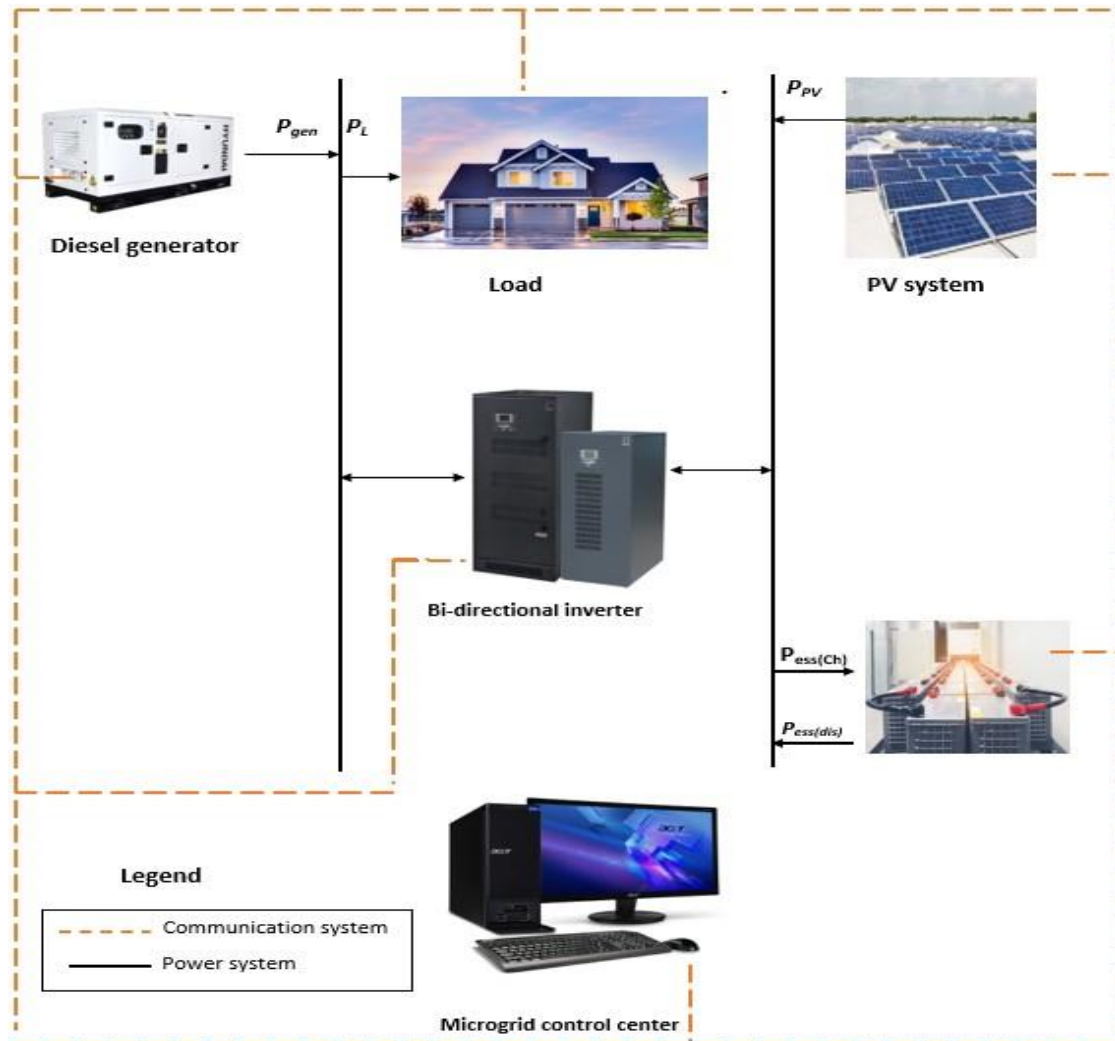


Figure 3.2: The proposed microgrid system of this study

3.1.2 Solar Resource Data

The study location is shown in Figure 3.3. Solar energy is one of Nigeria's most abundant commodities, as previously mentioned in chapter 1, since the sun shines throughout the year, with daily solar irradiance ranging from $4.14 - 5.74 \text{ kWh/m}^2$ [7].

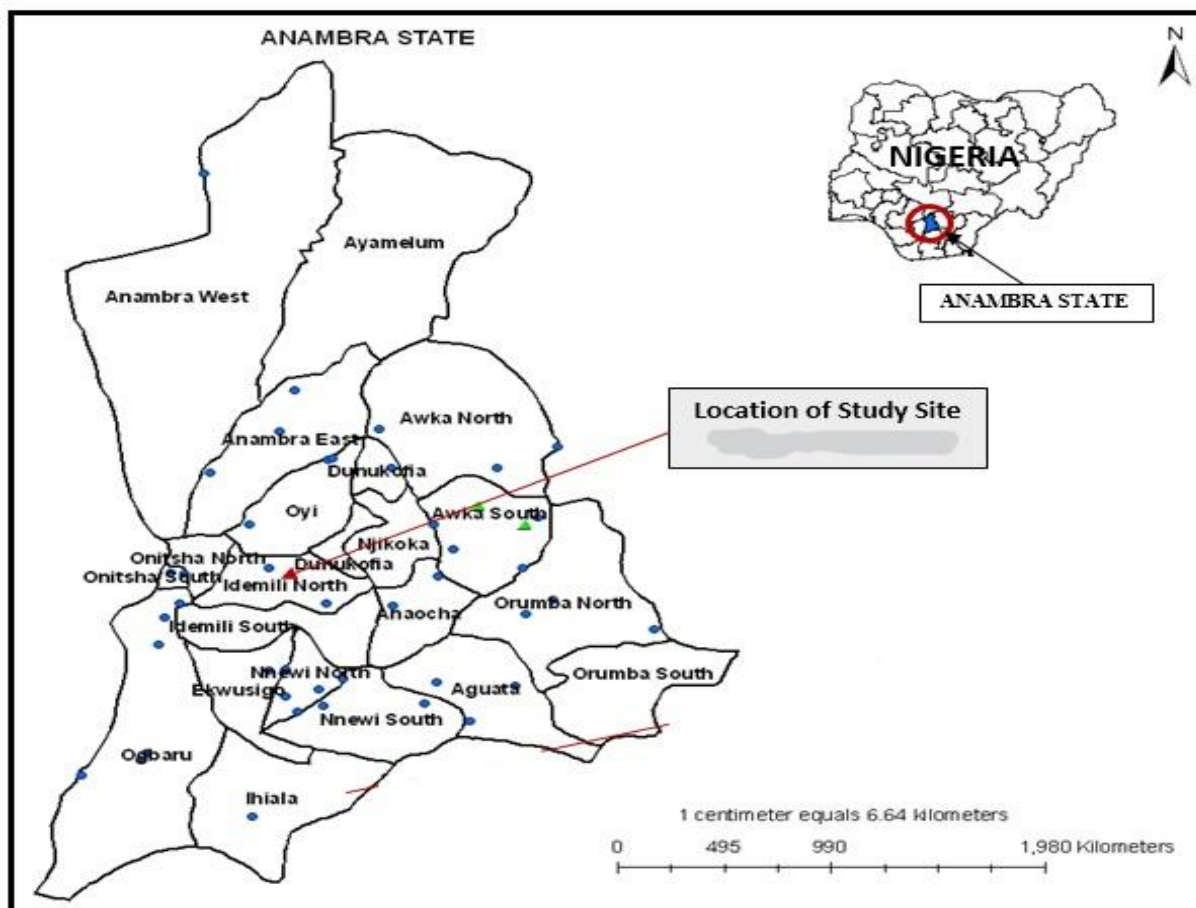


Figure 3.3: Map of Anambra State showing the location of the study area [7].

The amount of global solar irradiation that reaches the earth's surface in a typical year is depicted in solar resource data [57]. The community's monthly solar irradiance data were obtained from the National Aeronautics and Space Administration (NASA). The annual average solar irradiance at this location is $4.92 \text{ kWh/m}^2 / \text{day}$. The clearness index, which varies from 0 to 1, is the ratio of solar radiation on the earth's surface to solar radiation available at the top of the atmosphere. According to the data obtained from NASA and shown in Figure 3.4, the highest solar irradiance occurs in January, with a value of $6.0 \text{ kWh/m}^2 / \text{day}$. The lowest solar irradiance occurs in August, with a value of $3.8 \text{ kWh/m}^2 / \text{day}$. January, February, November, and December have the peak solar irradiance of the year. Furthermore, the annual average of the clearness index is 0.49; the highest clearness index is 0.59 in January and the lowest is 0.39 in August.

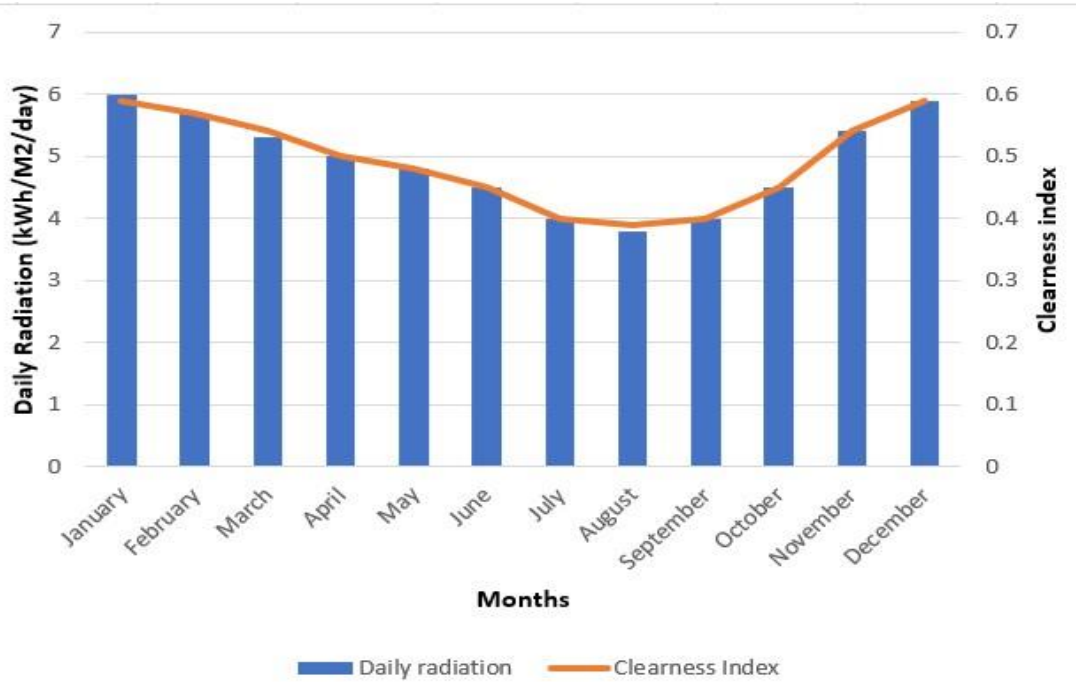


Figure 3.4: Solar resource data for the study area on a monthly average

3.1.3 Estimation of Load

The detailed analysis of all the community's appliances is shown in Table 3.1, while the total load demand of a typical household load in the community shown in Table 3.2. Several voltage levels can be considered for low voltage DC, including 48V, 120V and 230V. In the absence of a definitive standard, this study used a 48V DC stage. When the voltage is 48V DC, there is usually no need for direct contact protection [58]. The baseload is taken to be 19 kW, as shown in Figure 3.5.

Table 3.1: Total daily energy demand of all households in Ifite community

Load description	Qty	Load Current (A)	Load Voltage (V)	AC Load Power (VA)	Daily Duty Cycle (hrs/day)	Weekly Duty Cycle (days/wk.)	Power Conversion Efficiency (Decimal)	Nominal System Voltage (V)	Ampere-hour load (Ah/day)
Air conditioner	7	1.080	220	1662.50	4.07	1	0.85	48	165.84
Computer	21	0.250	220	1155.00	5.33	1	0.85	48	150.89
Electric fan	175	0.511	220	19687.50	4.81	1	0.85	48	2321.00
Electric iron	86	7.244	220	137062.50	0.05	1	0.85	48	167.97
Electric kettle	37	6.364	220	51800.00	0.07	0.142857	0.85	48	12.70
Electric oven	4	9.773	220	8600.00	0.29	0.142857	0.85	48	8.73
Energy saving bulb	375	0.064	220	5250.00	1.93	1	0.85	48	248.35
Food blender	36	1.455	220	11520.00	0.06	1	0.85	48	16.94
Freezer	7	0.900	220	1386.00	20.57	1	0.85	48	698.78
Hot plate cooker	35	5.795	220	44625.00	1.72	1	0.85	48	1881.25
Incandescent bulb	194	0.455	220	19400.00	3.09	1	0.85	48	1469.26
Microwave	5	3.636	220	4000.00	0.06	0.1322	0.85	48	0.78
Mobile phone	229	0.014	220	687.00	1.5	1	0.85	48	25.26
Radio/home theatre	39	1.000	220	8580.00	2.94	1	0.85	48	618.26
Refrigerator	34	0.705	220	5270.00	15.06	1	0.85	48	1945.25
Television	78	0.445	220	7644.00	6.41	1	0.85	48	1200.93
Video game	4	0.273	220	240.00	2.75	1	0.85	48	16.18
Washing machine	3	2.409	220	1590.00	1.5	0.1434	0.85	48	8.38
Water heater	8	9.091	220	16000.00	0.31	0.1223	0.85	48	14.87
Total AC load power (VA)				346159.50	Total Ampere-hour load (Ah/day)				2818.40

Table 3.2: The total daily energy demand of all households in Ifite community

Household appliance	Power Rating (W)	Number of Electrical Appliance	Total Power (kW)	Hours of use per day (hr/day)	Energy demand (kWh/day)
Air conditioner	1520	7	10.64	4.07	43.30
Computer/laptop	55	21	1.155	5.33	6.16
Electric fan	90	175	15.75	4.81	75.76
Electric iron	1275	86	109.65	0.05	5.48
Electric kettle	1400	37	51.8	0.07	3.63
Electric oven	2150	4	8.6	0.29	2.49
Energy saving bulb	14	375	5.25	1.93	10.13
Food blender	320	36	11.52	0.06	0.69
Freezer	198	7	1.386	20.57	28.51
Hot plate cooker	1275	35	44.625	1.72	76.76
Incandescent bulb	100	194	19.4	3.09	59.95
Microwave	800	5	4	0.06	0.24
Mobile phone	3	229	0.687	1.50	1.03
Radio/home theatre	220	39	8.58	2.94	25.23
Refrigerator	155	34	5.27	15.06	79.37
Television	98	78	7.644	6.41	49.00
Video game	60	4	0.24	2.75	0.66
Washing machine	530	3	1.59	1.50	2.39
Water heater	2000	8	18	0.31	5.58
Total					476.36

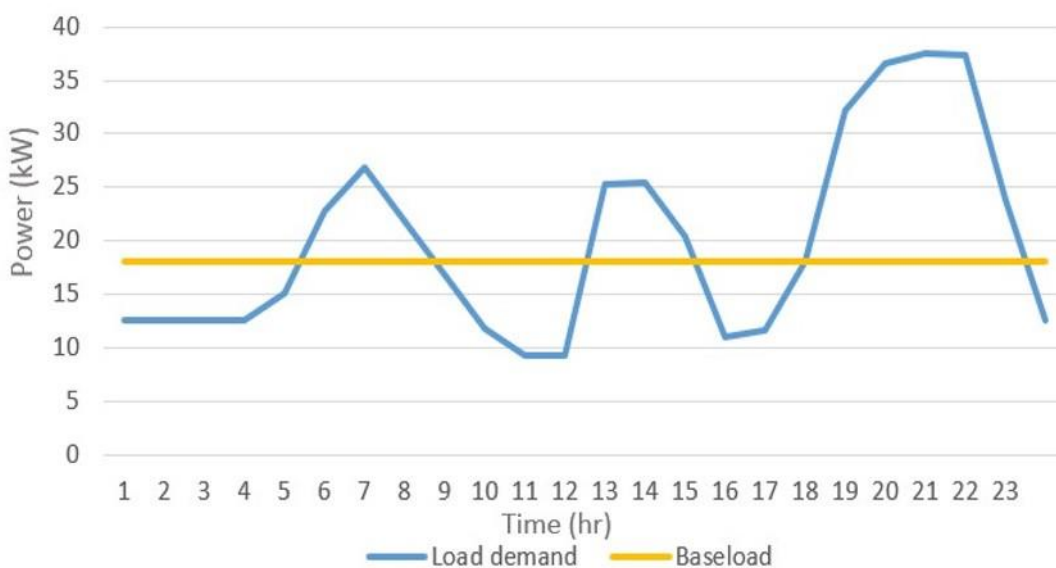


Figure 3.5: Load demand curve and baseload Profile

3.2 Analytical Design Calculation

3.2.1 Solar PV System

The optimum tilt angle for Nigeria, as studied in [59], is 10° . The monthly average solar irradiance for the latitude 10° is shown in Table 3.3. The solar irradiation a site would get if the sun shone at its brightest for a certain number of hours, called the peak sun hour (PSH), is also given in Table 3.3.

Table 3.3: The array tilt angle and the design current

Tilt angle 10°			
Month	Corrected Load (Ah/day)	Peak Sun (Hrs/day)	Design Current (A)
January	3195.46	4.36	186.87
February	3195.46	4.33	188.17
March	3195.46	4.23	192.62
April	3195.46	4.13	197.28
May	3195.46	4.04	201.68
June	3195.46	3.70	220.21
July	3195.46	3.85	211.63
August	3195.46	4.08	199.70
September	3195.46	4.31	189.04
October	3195.46	4.78	170.45
November	3195.46	4.89	166.62
December	3195.46	4.60	177.12

The largest design current with the lowest peak sun, 220.21 A, is used for the design calculation. This would ensure that the system would produce the necessary energy even on days when the sun is at its lowest peak, such as cloudy days. Another factor called the derating factor influencing the PV's output must be considered when designing this required current. Shade, soil, and manufacturing defects are all derating factors considered in this study for the PV. Consequently, the value of the derating factor in this study was set at 88% to ensure that the necessary current is delivered safely. Equation (3.1) is used to calculate the new calculated current when considering the derating factor. The number of PV modules in parallel will then

be determined using the newly calculated current and evaluated using Equation (3.2), while the number of PV modules in series is calculated using the DC system voltage and evaluated using Equation (3.3).

$$\text{The new calculated current} = \left(\frac{\text{Calculated current}}{\text{Derating factor}} \right) \quad (3.1)$$

$$\text{PV parallel connection} = \frac{\text{The new calculated current}}{\text{PV current}} \quad (3.2)$$

$$\text{PV series connection} = \frac{\text{DC system voltage}}{\text{PV voltage}} \quad (3.3)$$

Consequently, based on the parallel and series connections, the total number of PV modules required for this study is determined by Equation (3.4). The rated capacity of the PV is calculated by equation (3.5). The results of the above equations for the PV module requirement are shown in Table 3.4.

$$\text{Total PV modules} = \text{PV parallel connection} \times \text{PV series connection} \quad (3.4)$$

$$\text{PV rated Capacity} = \text{total number of PV module} \times \text{PV module capacity} \quad (3.5)$$

Table 3.4: The PV module requirement calculations

Peak Sun (hrs./day)	3.70	Nominal DC Voltage (V)	48
Calculated current (kA)	220.21	Rated Module Voltage (V)	34.6
Derating Factor (%)	88	Series Module Required	10
PV Current (A)	9.34	Total Modules	210
Parallel Module Required	21	PV array capacity for the load (W)	67,864.44

3.2.2 Inverter Selection

An inverter of 58 kW was chosen for the 70 kW PV system, which results in a 1.2 DC/AC ratio. A SUNSYS (model) 58 kW, 48V inverter with a built-in 55kW Maximum Power Point Tracking (MPPT) was chosen for this design. To meet the daily AC load demand for these PV capacities, the PV array output values must match the inverter input values given by the technical requirements of the inverter shown in Table 3.5. Furthermore, the inverter output must meet the AC daily load requirement. As a result, to meet the inverter input requirements, the PV modules were divided into sub-arrays, and the inverters were connected in parallel. PV voltage and current values are determined by the system's input specifications in general as

well as the inverter. Each PV module sub-array was measured using equations (3.6) for series connections and (3.7) for parallel connections.

Table 3.5: The technical specification for the selected inverter

Type		String bidirectional inverter
Model		SUNSYS-PCS2 IM 66TR
DC input	DC battery voltage	450 – 850
	Maximum charging current	160 A
	Maximum discharging current	160 A
AC output	Rated Power	66 kW
	Rated three-phase voltage.	400 V
	Rated frequency	50 Hz
Efficiency	Maximum efficiency	97 %

$$PV \text{ series sub – array connections} = \frac{V_{dc, inverter \text{ input, system voltage}}}{V_{pv, module}} \quad (3.6)$$

$$PV \text{ parallel sub – array connections} = \frac{I_{dc, inverter \text{ input}}}{I_{pv, module}} \quad (3.7)$$

The voltage input for the inverter was set to be equal to the DC system voltage of 560 V, and the input current was set to 1000 A, resulting in a maximum output of 550 kVA for the inverter. As a result, the following sizes were obtained:

- 1- The number of PV sub-array connections in series is 10, based on (3.6).
- 2- The number of PV sub-array connections in parallel is 21, based on (3.7)
- 3- The total number of PV sub-array is 210, based on (3.4)
- 4- The PV total sub-array capacity is calculated to be 67.9 kW, based on (3.5)

The number of parallel-connected inverters required was determined using Equation (3.8) and Table 3.4 since the maximum inverter output is 58 kW.

The inverter is connected to produce 67,520 W adequately, while the PV will output 67,864.44 W due to the PV array capacity to cover the daily community load by the solar PV system.

3.2.3 Battery Bank Sizing

Table 3.6 shows the Battery model, HUAFU, 24V, 450Ah deep cycle used for the design. This battery model is cheap and readily obtainable in Nigeria; it does not always require maintenance which is cost-saving. Deep cycle batteries have fast charging ability and discharge slowly. It has a reasonable maximum depth-of-discharge (DOD) in regard to other

battery design available. Battery manufacturers specify the maximum DOD of a battery. The DOD is defined as the dischargeable capacity from a fully charged battery divided by its nominal capacity. Equation (3.9) is used to calculate the battery bank capacity (C_B) required by the system [60, 61].

Table 3.6: Battery Specification

Make	HUAFU
Model	CN-6-500
Type	Deep Cycle
Nominal Voltage (V_B)	24
Rated capacity (Ah)	327

$$C_B = \frac{E_L \times DOA}{V_B \times DOD} \quad (3.9)$$

E_L is the daily load demand in kWh, DOA refers to "days of autonomy," which is the number of days the battery is supposed to supply electricity without getting a charge from the solar array. DOA is set to 2 days in this study's design.

V_B is each Battery's nominal voltage; it can be seen from Table 3.6 that V_B is 24 V.

DOD is the permissible depth-of-discharge limit, and this is set to 0.8.

When E_L , DOA, V_B , and DOD values are substituted in Equation (3.9), the required battery bank capacity is 8874.2 Ah.

Equation (3.10) was used to calculate the total number of batteries (N_{BT}), while equations (3.11) and (3.12) were used to calculate the number of batteries connected in series (N_{Bs}) and parallel (N_{Bp}), respectively.

$$N_{BT} = \frac{\text{Capacity of the battery bank}}{\text{Capacity of one battery}} = \frac{C_B}{C} \quad (3.10)$$

$$N_{Bs} = \frac{V_{DC}}{V_B} \quad (3.11)$$

$$N_{Bp} = \frac{N_{BT}}{N_{Bs}} \quad (3.12)$$

The total number of batteries required in series and parallel are shown in Table 3.7, which was obtained considering the battery bank capacity in Equation (3.9) and total number of batteries using Equation (3.10). The DOD of the HUAFU battery, as shown in Table 3.8, is 0.8, as stated by the manufacturer.

Table 3.7: Series and Parallel Battery Specifications

Nominal system voltage (V)	Nominal battery voltage (V)	Battery in series	Battery in parallel	Total batteries
48	24	2	76	152

Table 3.8: System Battery Capacity

Corrected Amp-hour Load (Ah/day)	Storage days	Maximum Depth of Discharge (Decimal)	Derate for Temperature (Decimal)	Required Battery Capacity (Ah)
3195.46	2	0.8	0.9	8874.21018

3.2.4 Diesel Generator Sizing

A microgrid system's diesel generator is designed for continuous operation, emergency standby power, short time running power, and prime running power [62]. Diesel generators are classified into three categories based on how they operate: continuous, prime, and standby. Continuous and prime power generators are quite similar because they all serve as the primary source of electricity and are designed to run constantly or over long periods of time. Continuous generator sets are designed to run continuously with a constant load, which is the main distinction between the two. On the other hand, prime generators are configured to supply a variable load for a long time. The standby/emergency generators, on the other hand, are only to be used while the utility grid is down. The prime generator is used in this study; the manufacturer designed it to adapt rapidly to load fluctuations [63]. The diesel generator operates at 30–90% of the manufacturer's nominal output. This study considers a diesel generator with a rating of 65 kVA that supplies the load (64.04 kW peak) with a total power capacity of 58 kW. The generator's output power was assumed to have a power factor of 0.9 in this study. The capacities of the proposed microgrid modules are shown in Figure 3.6. The power generated by the diesel generator can be estimated using Equation 3.13.

The generator model is given by equation (3.13)

$$P_{gen} = P_n \times N_{gen} \times \eta_{gen} \quad (3.13)$$

where P_{gen} is the power generated (kW); P_n is the nominal power generated by the diesel generator (kW); N_{gen} is the number of diesel generators; and η_{gen} is the efficiency of the diesel generator.

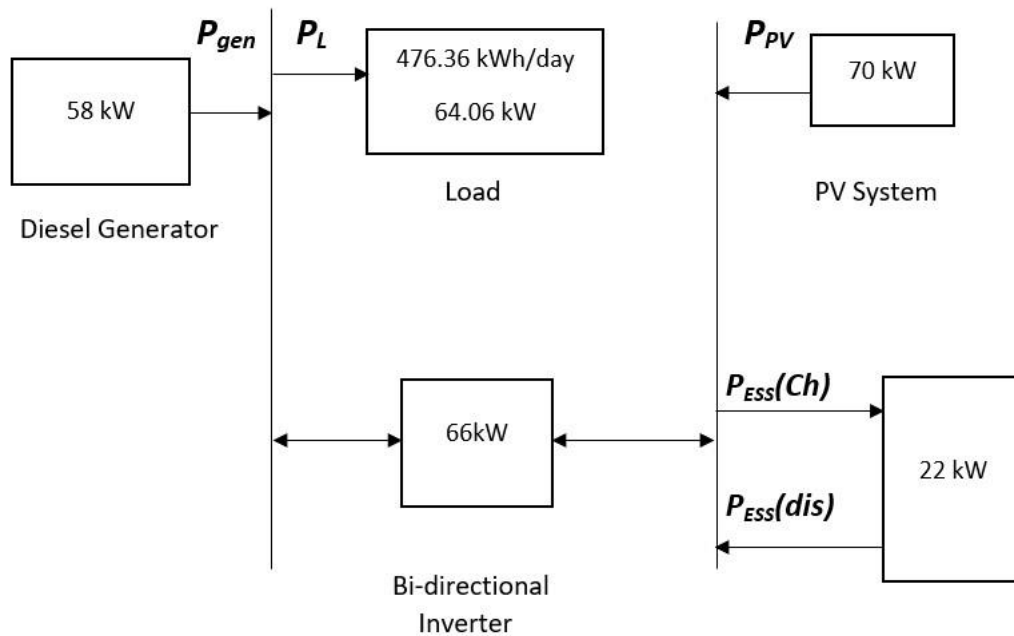


Figure 3.6: Capacities of the proposed microgrid components

Table 3.9: The proposed Microgrid System's technical and financial parameters

Component	PV	Inverter	Battery	Generator
Rating of each component	325 W	66 kW	12V, 327 Ah	60 kVA
Required No of components	210	1	152	1
Final rating	70 kW	58 kW	48 V, 21580 Ah 1035936kWh, 21.6 kW	58 kW

3.3 Simulation and Analysis using HOMER Pro Software

Sizing and optimizing a standalone PV device can be done by various tools. HOMER is software used for studying, sizing, and analyzing data of various PV systems [64]. It is a reliable software for predicting the overall performance of a standalone PV system under real-world conditions [65]. The simulation process was carried out in this paper using HOMER

software. The layout of the standalone PV system in HOMER pro software is seen in Figure 3.7.

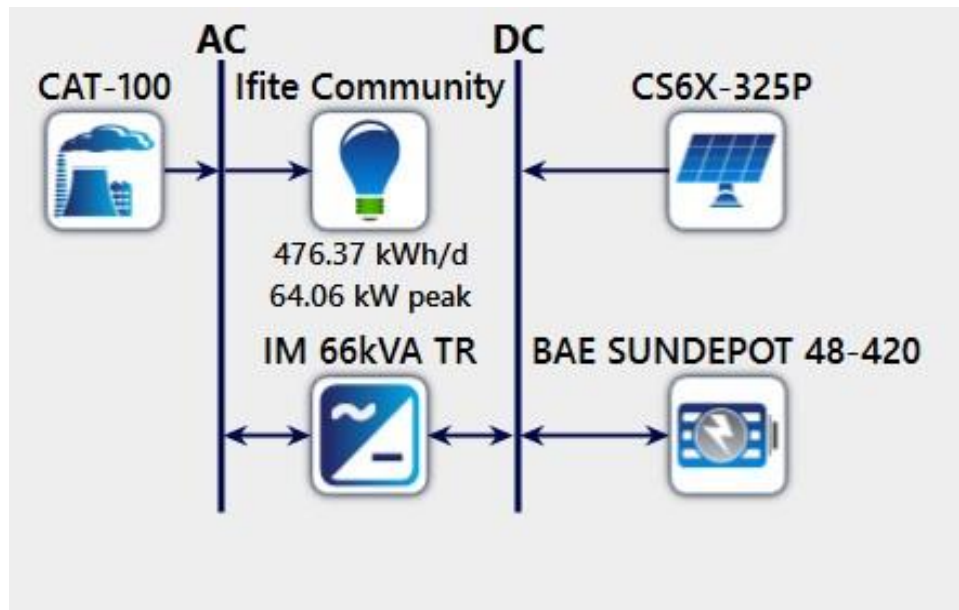


Figure 3.7: HOMER Schematic for the proposed Microgrid

The configuration is made up of Load, PV, inverter, and Battery. As discussed in the analytical calculations, the PV kilowattage sizing has been chosen in HOMER to be 70 kW to support the diesel generator's capacity to supply the load demand. These ratings are based on technical parameters as well as the PV and inverter's analytical calculations.

The PV modules tilt angle of 10° and orientation of the South-west were considered in the HOMER tool system performance analysis.

3.3.1 Solar PV Module

During daytime hours, the solar PV panels for the system configuration provide power to the load while charging the batteries. The peak demand during daylight hours, at 9 PM, was determined to be 36 kW, as shown in Figure 3.1. The total PV capacity was set at 70 kW, and a derating factor of 88% was applied for the configuration. This factor decreases the electricity production of the solar PV panel by 12%. The derating factor include factors such as panel soiling, shading, ageing, and wiring losses. The solar PV module power output P_{pv} (kW) is a function of the cell temperature and solar irradiance and is calculated by HOMER using Equation (3.14).

$$P_{pv} = P_{rated} * f_{pv} * \left(\frac{G_T}{G_{T,STC}}\right) * [1 + \alpha_p(T_C - T_{C,STC})] \quad (3.14)$$

where P_{rated} is rated capacity of the PV array (kW); f_{pv} is the PV derating factor; G_T is solar radiance incidence on the PV array (kW/m²); $G_{T,STC}$ is the incident radiation at standard test conditions (1 kW/m²); α_p is the temperature coefficient of power; T_c is the cell temperature of PV; $T_{c,STC}$ is the cell temperature of PV under standard test conditions (25°C).

A Canadian solar PV module CS6X-325P was selected from HOMER library for this model. The chosen model is a polycrystalline type, and it is relatively cheap. The characteristics of the PV module obtained from the manufacturer's datasheet are shown in Table 3.10.

Table 3.10: PV Module specification

Cell type	Polycrystalline
Model	CS6X-325P
Nominal maximum Power (P_{max})	323 W
Optimum operating voltage (V_{mp})	34.0 V
Optimum operating current (I_{mp})	8.78 A
Open circuit voltage (V_{oc})	34.6 V
Short circuit current (I_{sc})	9.34 A
Module efficiency	16.94 %
Temperature coefficient (P_{max})	-0.41 %/ °C
Temperature coefficient (V_{oc})	-0.31 %/ °C
Temperature coefficient (I_{sc})	0.053 %/ °C
Nominal operating cell temperature (NOCT)	45 ± 2 °C

3.3.2 Sizing of Inverter

The load demand is connected to the AC bus, while the PV module is connected to the DC bus. Therefore, the system would need an inverter to convert the PV power into AC to supply the required load. As a result, an inverter of the type SMA-SC500HE grid-tied inverter 3-Phase 58 kW was selected for this system to meet the 64 kW peak load [66]. The inverter has a 5-year warranty; therefore, the inverter's chosen lifetime is 5 years.

3.3.3 Battery Sizing

A lead-acid battery was considered for the model. The Battery, a BAE SUNDEPOT 24-420, rated 327Ah (7.85kWh) and was selected from HOMER library. The model is configured with two batteries connected in a series string and 76 batteries connected in parallel. The battery specification selected is shown in Table 3.11.

Table 3.11: Battery Specification

Type	Lead-acid
Model	8CS25P
Nominal voltage	8 V
Nominal capacity	1156 Ah
Maximum capacity	1186 Ah

The lifetime of a battery bank is defined by the depth of discharge and cycles to failure. The depth of discharge is the fraction of the battery that has been discharged to the Battery's total capacity [67]. The battery lifetime R_B (years) is calculated by HOMER using equation (3.15).

$$R_B = \min \left(\frac{N_B \cdot Q_{lifetime}}{Q_{throughput}} R_{B,f} \right) \quad (3.15)$$

where N_B is the number of batteries; $Q_{lifetime}$ is the lifetime throughput of the battery (kWh); $Q_{throughput}$ is the annual battery throughput (kWh/year); and $R_{B,f}$ is the battery's float life.

3.3.4 Diesel Generator

The diesel generator used in this study has a total power capacity of 58 kW and a rating of 65 kVA. Since HOMER Pro only deals with kilowattages ratings (real Power), the power factor for the generator's output power was chosen to be 0.9 in this study. As a result, in order to simulate in HOMER, converting kVA to kW is needed. In this study, the diesel generator was used in all the six scenarios. HOMER Pro contains a variety of generic generators of various sizes. However, a small generic generator was used in the simulation and modified to meet this study's criteria.

3.4 MATLAB Software Analysis

3.4.1 Problem Formulation

The study's main objective was to improve the proposed microgrid's reliability (RI) while lowering the Annual System Cost (ASC) and Cost of Energy (COE) as well as meeting the electricity demand of the community. As a result, the first aspect of the objective function was to reduce the cost of electricity and the annual system's cost while meeting the microgrid system constraints and the consumer's power demand, as shown in Equation (3.20). The

second part of the objective function was formulated to minimize the PV and ESS reliability index in the proposed microgrid system, as shown in Equation (3.21).

$$F = \min \sum_{i=1}^n (COE + ASC) \quad (3.20)$$

$$F = \max \sum_{i=1}^n (RI) \quad (3.21)$$

Subject to

$$\left\{ \begin{array}{l} P_{gen}^{min} \leq P_{gen} \leq P_{gen}^{max} \\ P_{PV}^{min} \leq P_{PV} \leq P_{PV}^{max} \\ P_{BESS}^{min} \leq P_{BES} \leq P_{BES}^{max} \end{array} \right. \quad (3.22)$$

where the first component of the objective function in Equation (3.22) of the proposed microgrid is the cost of the energy generated by the proposed microgrid system, expressed in Equation (3.23)

$$\text{Cost of Energy (COE)} = \frac{\text{Annual Cost of the System (ACS)}}{\text{Annual Electricity Produced (AEP)}} (\$/kWh) \quad (3.23)$$

The objective function's second element, which is the Annual System Cost (ASC), is the sum of Annual Fuel Cost (AFC), Annual Maintenance Cost (AMC) and Annual Operation and Maintenance Cost (OMC) as expressed in Equation (3.24), and previously discussed in section 2.7.

$$ASC = (AFC + AMC + OMC) (\$/year) \quad (3.24)$$

The objective function's third element is the Reliability Index, as shown in Equation (3.25), and previously discussed in section 2.7.

$$RI = EENS \times K_e (\$/yr) \quad (3.25)$$

where EENS is the Expected Energy not Served; K_e is the value of the lost load.

The simulation was performed using the fmincon tool in MATLAB to study the PV integration effect on the cost and reliability of the microgrid, and HOMER software was used to show the

feasibility and the operation strategy. These models were applied to six scenarios, and the results were compared to a scenario where a diesel generator alone was used to meet the same load demand.

3.5 Constraint functions

The multi-objective functions proposed in this study were subjected to constraints that were designed to keep them operating within their defined minimum and maximum limits. The proposed microgrid system considers the power balance, ESS, SOC, and power generation constraints. The following are the system constraints that were considered in this study:

3.5.1 Constraint on power balance

The power generated by various sources, such as the diesel generator, PV, and ESS units, was designed to meet system load demands on a continual basis. Equations (3.26) and (3.27) are used to express the power balance.

$$P_L(t) = P_{PV}(t) - P_B(t) + P_{DG}(t); \text{ for day (9 am-5 pm)} \quad (3.26)$$

$$P_L(t) = P_B(t) + P_{DG}(t); \text{ for night (6 pm – 8 am)} \quad (3.27)$$

where P_L is the load point power demand; P_{DG} is the diesel generator generated power; P_{PV} is the PV system power system; P_{BC} is the battery charging power; P_{BD} is the battery discharging Power.

3.5.2 Constraints on output power

The generator, PV, and BES power outputs at time (t) should all be able to operate within their specific minimum and maximum limits. The output power of each generation source has minimum and maximum limits, as shown in equation (3.22). Each power source's power flow cannot be negative or exceed its maximum allowable value.

3.6 Configuration of the case study

Various scenarios are investigated and studied to have a thorough knowledge of the effects of PV-BES in the DG microgrid system. As a result, the effects of PV-BES on the DG system can be examined using the following scenarios:

- Scenario One

The diesel generator has a rating of 58 kW, the maximum power limit of the diesel generator P_{gen}^{max} is 58 kW while the minimum output power P_{gen}^{min} is 0 kW (the generator operates at 30-90% of its rated power). In this scenario, the total community load is solely supplied by the generator; there is no power output from the PV and battery in this scenario.

- Scenario Two

The maximum PV output power P_{PV}^{max} in this scenario was set at 15 kW. The PV power output depends on the irradiance data obtained from NASA. Furthermore, the maximum power of the battery P_{BESS} was set to 0 kW. Therefore, the generator power output P_{Gen} at all times depends on PV total output power.

- Scenario Three

The maximum PV power output P_{PV}^{max} in this scenario was set to 30 kW, while the minimum and maximum power output of the battery P_{BESS}^{max} was set to 5kW. Therefore, the P_{Gen} depends on the power output of the PV and Battery.

- Scenario Four

In this scenario, the P_{PV}^{max} was set to 45 kW, also the P_{BESS}^{max} was set to 10 kW. The diesel generator compensates for the deficiency of the PV output power and battery. Therefore, the generator output power always depends on the power output from the PV and Battery.

- Scenario Five

The P_{PV}^{max} was set to 60 kW in this scenario; also, the P_{BESS}^{max} was set to 15 kW. The diesel generator compensates for the deficiency of the PV output power and battery. Therefore, the power output from the generator always depends on the PV output power and Battery.

- Scenario Six

In this scenario, the P_{PV}^{max} was set to 70 kW, also the P_{BESS}^{max} was set to 22 kW. The diesel generator compensates for the deficiency of the PV power and battery. Therefore, the generator output power always depends on the PV output power and battery.

3.7 Proposed Microgrid Algorithm

The `fmincon` function in MATLAB optimization tool is used to solve the non-linear optimization problem of a microgrid system. To solve this study's multi-objective problems, the `fmincon` solver from the MATLAB R2016b optimization toolbox was utilized. The study's objective function is expressed in Equation (3.28).

$$\begin{cases} A_{eq} \cdot X = B_{eq} \\ L_b \leq X \leq U_b \end{cases} \quad (3.28)$$

where $L_b \leq X \leq U_b$ is the lower and upper bounds of the DG, PV and Battery in the six scenarios as shown in Table 3.13.

$A_{eq} \cdot X = B_{eq}$ is the linear equality constraint = final/maximum load demand of the community.

Table 3.12 details the technical specification and costs for each microgrid system component [68]. The PV unit's economic feasibility in a power system was determined using these technological and financial details. Using the configuration of scenarios outlined in Table 3.13, the `fmincon` optimization technique described in this section was applied to the proposed MG system.

Table 3.12: The microgrid system's technical and cost parameters [31, 68]

Components	Capital Cost	Replacement Cost	Failure Rate	Maintenance	Lifetime
Diesel generator	300 \$/kW	300 \$/kW	0.06	0.013 \$/kW/yr	25,000 hr
PV	550 \$/kW	550 \$/kW	0.03	\$10 \$/kW/yr	25
Battery	300 \$/battery	300 \$/battery	0.04	10 \$/battery/yr	5 yrs
Inverter	300 \$/kW	300 \$/kW	0.03	3 \$/kW	15 yrs

Table 3.13: Configuration of Scenarios

Scenario	Diesel generator capacity (kW)	PV integration level (kW)	Battery integration level (kW)
1	58	0	0
2	58	15	0
3	58	30	5
4	58	45	10
5	58	60	15
6	58	70	22

3.8 Microgrid system's Reliability Indices

The loss of load probability (LOLP) is a probabilistic measure of the load's unavailability within a specified period. Based on the size of the system under evaluation and the extent of input data (generation availability model, outage probability and load data) available. The LOLP calculation methodology proposed in this thesis was calculated by utilizing the capacity outage probability table (COPT), failure rate (FR) and load duration curve (LDC). The load duration curve of the load profile of the study area is shown in Figure 3.8. Tables 3.14 - 3.16 show the COPT of the Diesel generator, PV, battery, while Table 3.17 shows the COPT of all the units. Figure 3.9 shows a flowchart describing the step-by-step approach of the proposed LOLP calculation methodology. The cost of load loss (CLL), loss of load probability (LOLP), expected energy not served (EENS) and the loss of load expectation (LOLE) was calculated by Equations 2.1 – 2.4. The MATLAB codes for the COPT calculation can be found in appendix (A), while the MATLAB code for the LOLP, CLL, EENS and LOLE calculations is provided in appendix (B).

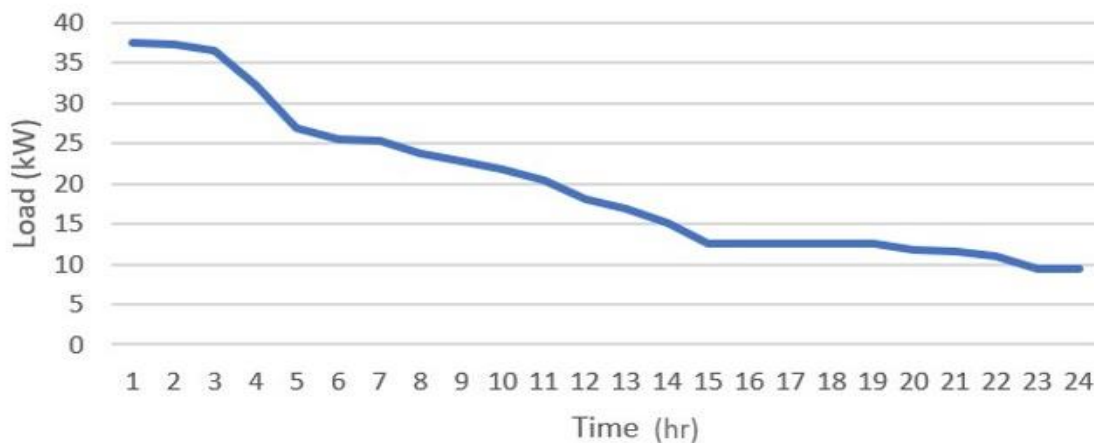


Figure 3.8: Load Duration Curve of Ifite Community

Table 3.14: COPT for diesel generator

Capacity Available	Capacity Unavailable	State Probability	Cumulative Probability
58	0	0.06	1.0
0	58	0.94	0.94

Table 3.15: COPT for PV

Capacity Available	Capacity Unavailable	State Probability	Cumulative Probability
70	0	0.03	1.0
0	70	0.97	0.97

Table 3.16: COPT for the Battery

Capacity Available	Capacity Unavailable	State Probability	Cumulative Probability
22	0	0.04	1.0
0	22	0.96	0.96

Table 3.17: COPT of all the Units

Capacity Available	Capacity Unavailable	State Probability	Cumulative Probability
150	0	0.00007200	1.00000000
128	22	0.00172800	0.99992800
92	58	0.00112800	0.99820000
80	70	0.00232800	0.99707200
70	80	0.02707200	0.99474400
58	92	0.05587200	0.96767200
22	128	0.03647200	0.91180000
0	150	0.87532800	0.87532800

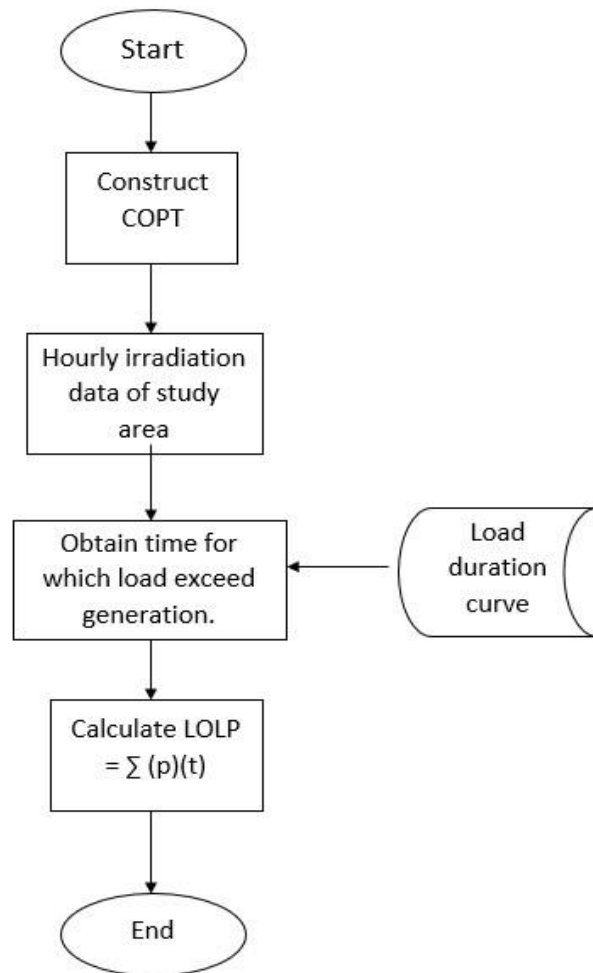


Figure 3.8: Flowchart for the LOLP calculation methodology

Figure 3.9 shows the research methodology's sequential flow chart. The technical and cost details were utilized to evaluate the PV system's economic feasibility in a microgrid system. The developed model evaluated the yearly cost, cost of energy, and reliability indices of integrating the PV system in the proposed microgrid system by employing technical specifications, reliability indices, and cost parameters. The MATLAB code for economic modelling can be found in appendix (C).

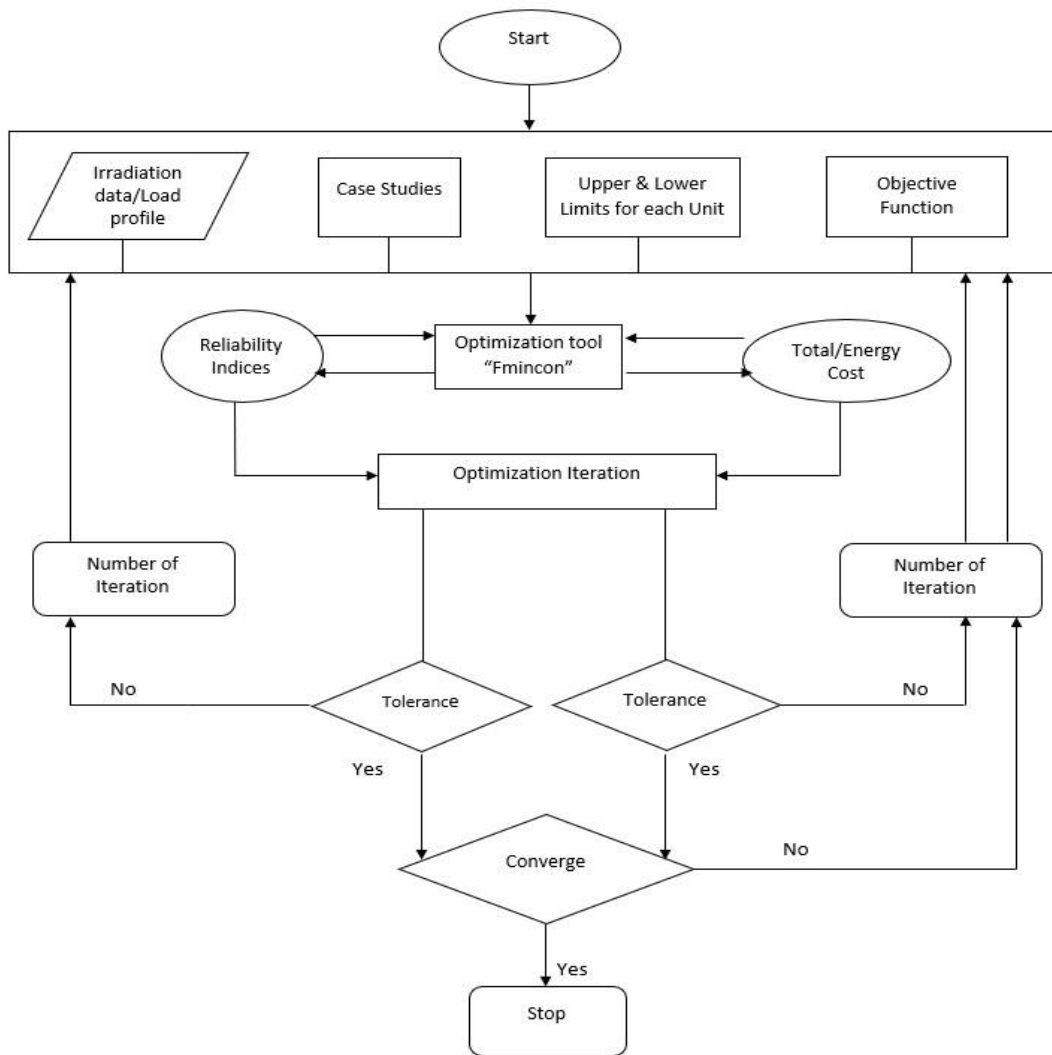


Figure 3.9: Research Methodology Flow chart

3.9 Summary

As the selected case study, Ifite community in Anambra state, Nigeria has the following load profile: 476.36 kWh with a peak load of 64 kW and a base load of 19 kW. This load will be supplied by the diesel generator and the proposed PV-BES system concurrently. Analytical design calculations are completed after choosing a DG model, PV module and a battery model to be used for the proposed DG-PV-BES system. Hence, these calculations result in having capacities of 58 kW DG, 70 kW PV, 66 kW inverter and 22 kW battery. The analytical result calculation was inputted in HOMER Pro software to confirm the feasibility of the analytical calculation results. Fmincon optimisation function in MATLAB used to solve the non-linear optimisation problem of the microgrid system was discussed. Also, the constraints function on the various case studies configuration are detailed.

Chapter 4 Results and Findings

4.0 Overview

The simulation results of the PV-DG-BES and their discussions are presented in this chapter. The simulation results of six scenarios are discussed, and the system reliability and economic analysis throughout the year are examined. The results obtained from the study were analysed to determine the effects of PV-BES variations on the optimal operation of the proposed microgrid system. The PV system's effect was used as a benchmark to assess its reliability and economic benefits in a microgrid system. Furthermore, a comparison analysis between the six scenarios in terms of economics, specifically in three main aspects, namely, the total NPC, LCOE and the annual operating costs was done. Also, the six scenarios' reliability was compared in the following aspects: the LOLP, LOLE, EENS, and Cost of Load Loss.

4.1 Configuration of Scenarios

The configurations of the considered scenarios in this study are presented in Table 3.13. Table 3.13 highlights the diesel generator (DG) installed capacity and the PV-BES various integration level in the scenarios. Generally, the DG operation level decreases as more solar PV-BES are incorporated into the microgrid system. Equations (2.5), (2.6) and (2.9) were used to evaluate the values of NPC, LCOE and AFC, respectively, obtained in Table 4.1. The resulted values, which are the economic analysis results of the scenarios' configuration presented in Table 3.13, are presented in Table 4.1.

Table 4.1: Economic analysis results of the Scenarios

Scenario	Initial Capital Cost (\$)	AFC (\$/yr.)	NPC (\$)	LCOE (\$/kWh)
1	88,218	55,837	811,519	0.255
2	113,518	54,430	819,966	0.261
3	139,518	41,764	715,616	0.231
4	154,968	35,351	664,775	0.217
5	170,418	32,334	657,929	0.218
6	192,118	24,608	614,191	0.209

Furthermore, the proposed microgrid system's reliability assessment was also calculated by using Equations (2.1) – (2.4). The loss of load probability (LOLP) was evaluated by using Equation (2.1), considering the capacity outage probability (COP) values in Tables 3.15 – 3.18 and the hourly solar irradiance of the study location. The LOLP was obtained by Equation (2.1) utilising the COP values in Tables 3.15 – 3.18 and the hourly solar irradiance of the study location. The Loss of Load Expectation (LOLE) and the Expected Energy Not Served (EENS) were evaluated by using Equations (2.2) and (2.3), respectively, using the hourly solar irradiance data and the COP values in Tables 3.15 – 3.18. Figures 4.1 to 4.4 show the LOLP, LOLE EENS, and cost of load loss, respectively, for the considered microgrid system scenarios.

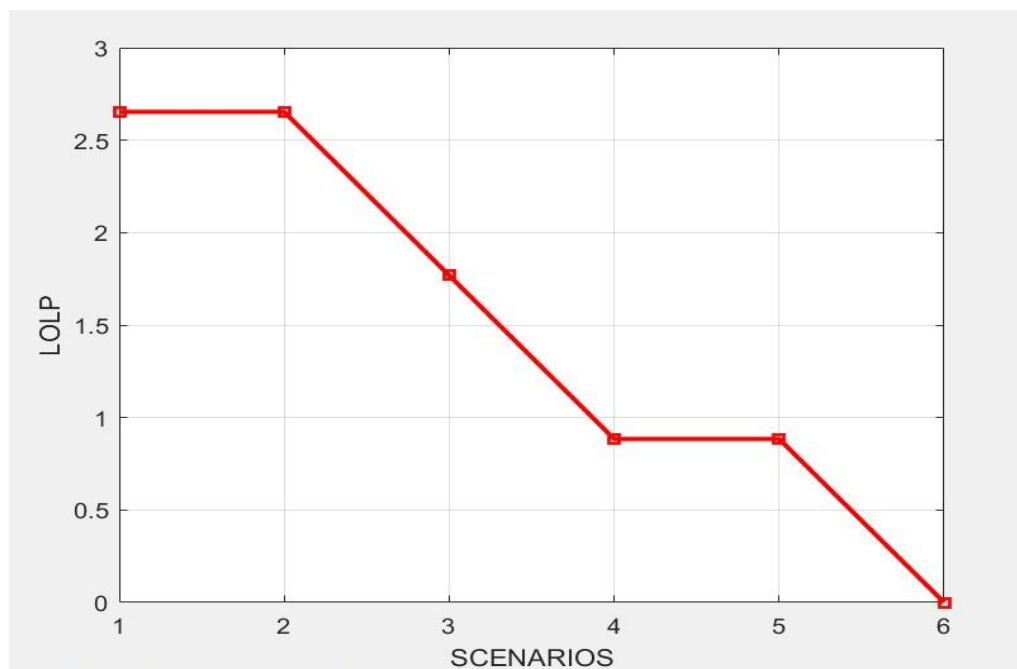


Figure 4. 1: Loss of Load Probability Results for the Scenarios

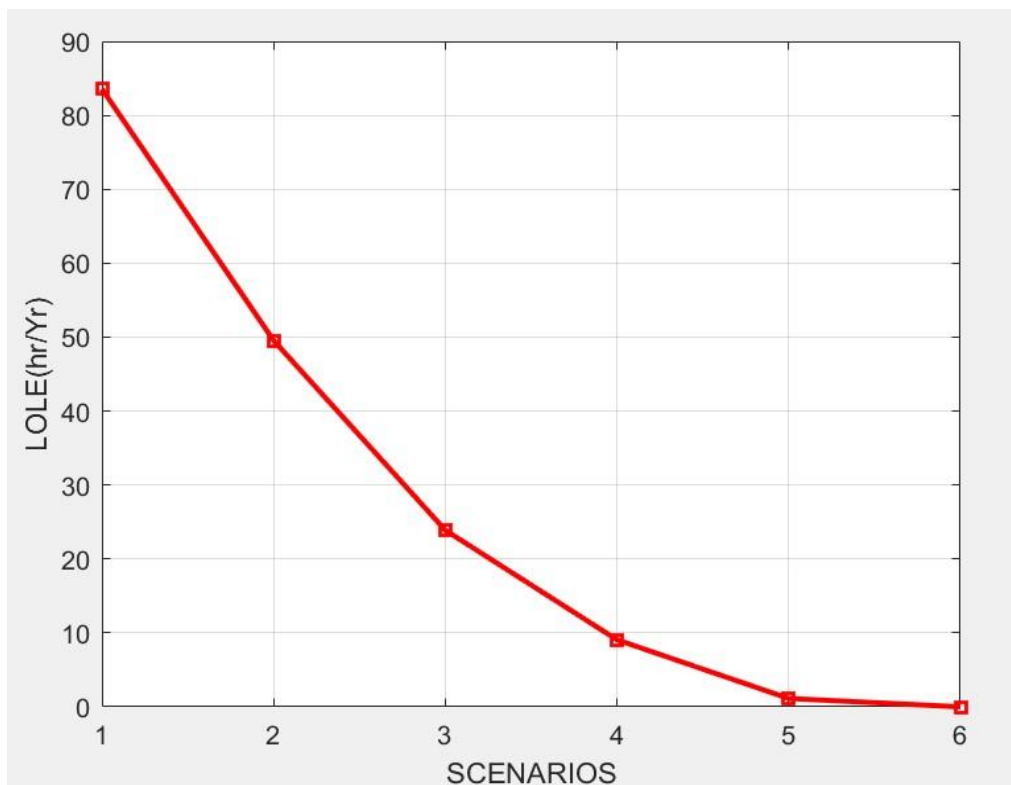


Figure 4.2: Loss of Load Expectation Results for the Scenarios

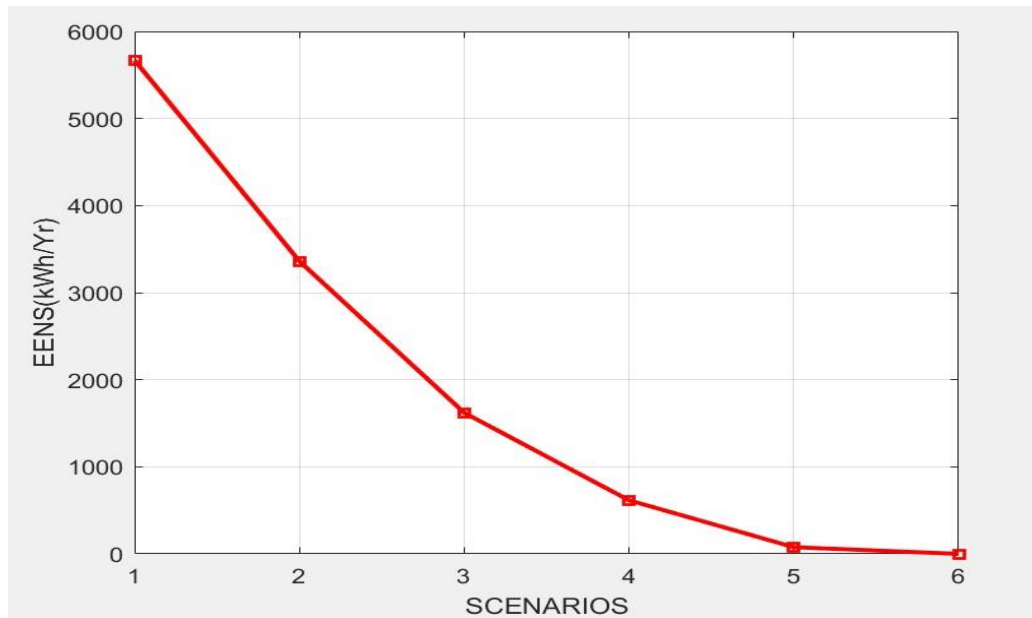


Figure 4.3: Expected Energy Not Served Results for the Scenarios

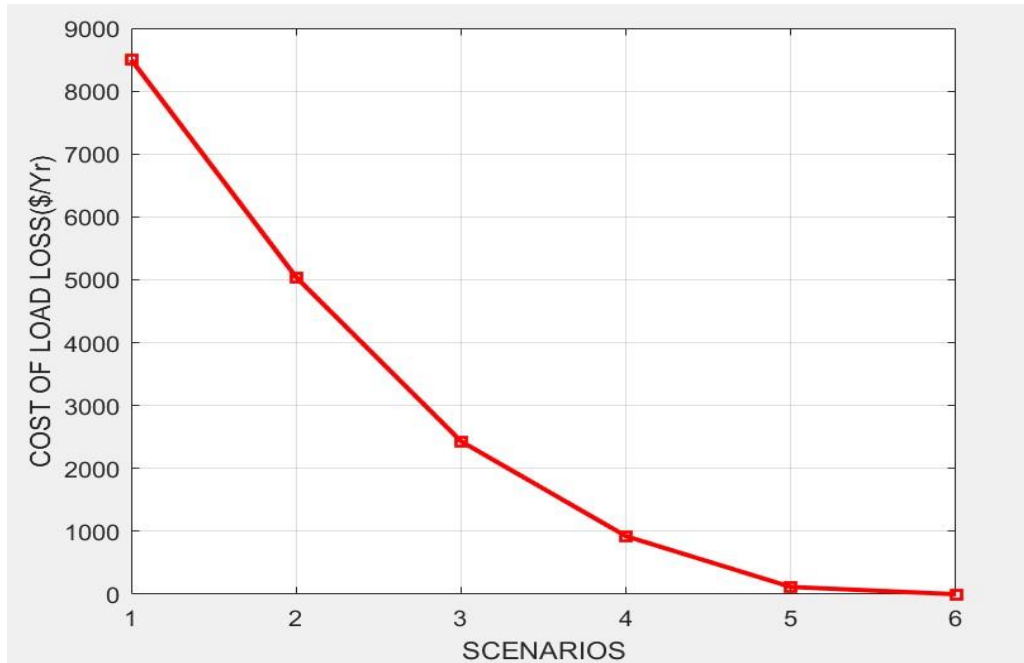


Figure 4.4: Cost of Load Loss Results for the Scenarios

The Load Following (LF) dispatch strategy was chosen in the HOMER tool to provide the optimum results. The load following strategy is a dispatch strategy whereby the generator produces only enough power to meet the primary load whenever it operates. Lower-priority objectives such as charging the storage bank or serving the deferrable load are left to renewable sources.

4.1.1 Scenario 1

In scenario one, the diesel generator solely meets the community's load demand since no other power source is operational. The variation of the load demand and power from the diesel generator is shown in Figure 4.5. Figure 4.5 shows that the diesel generator meets the total load demand at all times of the day in the considered location. This is mainly because the diesel generator system is sized to ensure that the considered energy demand is always supplied.

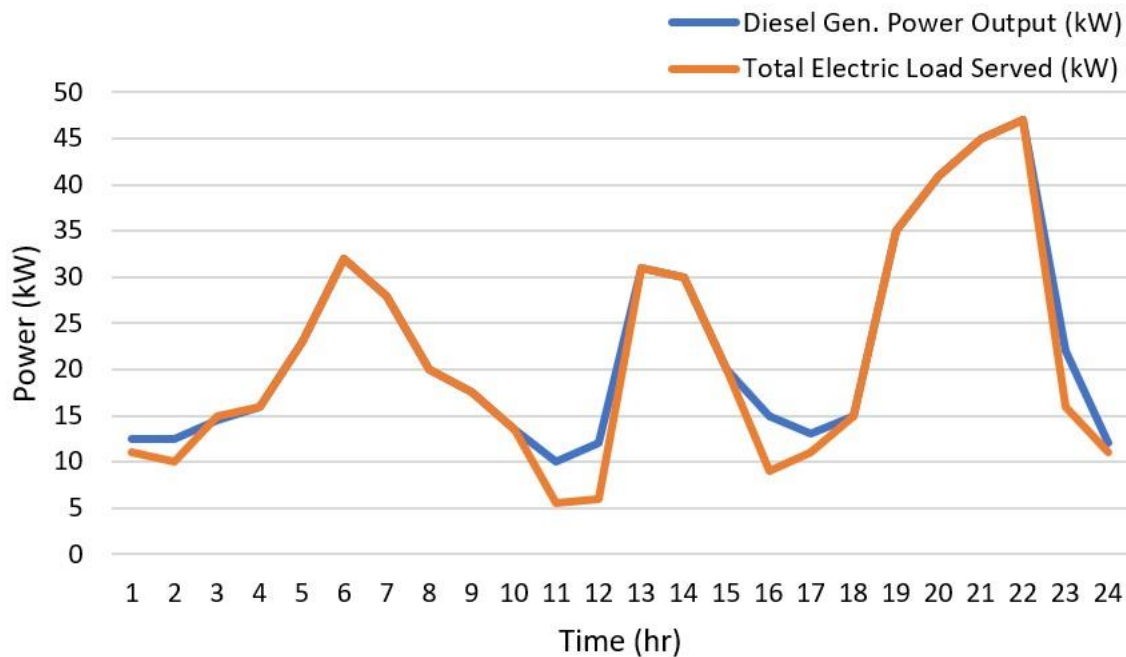


Figure 4.5: Variation of power from DG and load demand and for Scenario 1

In this scenario, the diesel generator's net present cost (NPC) is \$811,519 with a levelized cost of energy (LCOE) of 0.255 \$/kWh and an annual fuel cost (AFC) of 55,837 \$/year. The cost-effectiveness of the diesel generator depends on the daily power demand of the end-users since there is no alternative to complement its operation. The value of the LOLP obtained is 2.6, as shown in Figure 4.1. The LOLP value obtained indicates a high probability that the daily peak load or the hourly demand will sometimes surpass the DG capacity. The values of LOLE and EENS results obtained for scenario one is 84 hr/year and 5800 kWh/year, respectively, as shown in Figure 4.2 and 4.3. The value of the cost of load loss obtained by using Equation (2.4) is 8,700 \$/yr., as shown in Figure 4.4.

4.1.2 Scenario 2

This scenario utilises the diesel generator of 58 kW rating and 15 kW PV (without BES) to meet the consumer load demand as described in Table 3.13. The PV generating units run simultaneously with the diesel generator to supply electrical power to the load points. The behaviours and contribution of each generating unit for 24 hours are presented in Figure 4.6a.

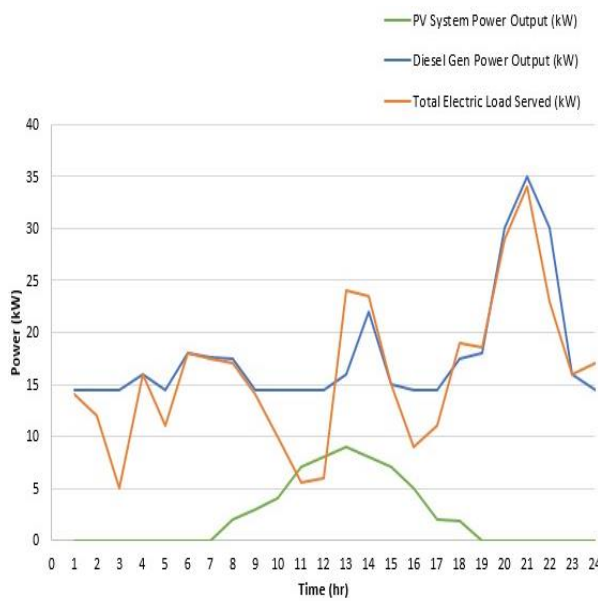


Figure 4.6a: Variation of power from PV-DG & load demand for Scenario 2

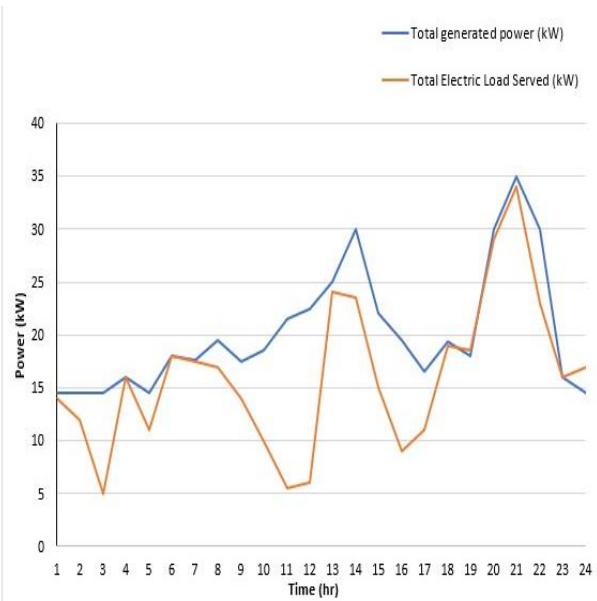


Figure 4.6b: Aggregate power from PV-DG and load demand for scenario 2

It is observed from Figure 4.6a that the diesel generator power has been reduced owing to the integration of 15 kW PV units into the system. The PV system contributed about 8 kW to the load demand between 10:00 to 14:00, but its capacity is small to contribute to the system significantly. Also, the aggregate power from PV-DG and electric load demand is shown in Figure 4.6b. The economic analysis results of scenario 2 presented in Table 4.1 and the reliability evaluation results obtained in Figures 4.1 to 4.4 show that the system's performance and cost saving improved slightly compared to scenario 1 where the diesel generator alone meets the load demand.

The values of NPC, LCOE and AFC for scenario 2 were obtained by using Equations (2.5), (2.6) and (2.9), respectively. The NPC, LCOE and AFC values obtained in Table 4.1 are the economic analysis results of the scenario 2 configuration presented in Table 3.13. This scenario's net present cost (NPC) is \$819,966 with a levelized cost of energy (LCOE) of 0.261 \$/kWh and an annual fuel cost (AFC) of 54,430 \$/year. The value of the LOLP obtained is 2.6, as shown in Figure 4.1. The LOLP value of this scenario is the same as for scenario 1, indicating that no significant improvement is made in generation system capacity. The LCOE in this scenario is higher than LCOE of scenario 1 because the installed PV panels are small to make a significant impact on the energy generated. The cost of load loss value obtained by using Equation (2.4) is 5000 \$/yr, as shown in Figure 4.4. The cost of load loss (CLL) value obtained in this scenario

is less than the CLL value obtained in scenario 1, showing that the cost of electric outage is reduced in this scenario due to the reduced outage time.

The LOLE and EENS results obtained are 50 hr/year and 3200 kWh/year, respectively, as shown in Figures 4.2 and 4.3. The loss of load expectation (LOLE) value obtained in this scenario is less than the LOLE value obtained in scenario 1. Therefore, the expected outage hours have reduced from 84 hr/year to 50 hrs/year. Also, The expected energy not served (EENS) Value in this scenario is less than the EENS in scenario 1, showing a reduction in the total energy not delivered to the load.

4.1.3 Scenario 3

The economic and reliability evaluation were performed further to assess the effect of PV - BES in the proposed microgrid system by adding more PV and BES units to the DG, as presented in Table 3.13. As a result, 30 kW PV and 5 kW BES units were incorporated into the microgrid system in this scenario. The PV-DG-BES system run simultaneously to meet the community's load demand. As shown in Figure 4.7a, the power produced by each generating unit indicates that the diesel generator's power output and operational time have further reduced with the integration of an additional number of the PV and ESS units. Figure 4.7a shows that between 11:00 to 19:00, the diesel generator did not operate at all. It can be seen from Figure 4.7b that the aggregate power supplied by the PV-DG-BES met the load demand at all time. The net present cost (NPC) of all the proposed microgrid technologies diesel generator in this scenario is \$715,616 with a levelized cost of energy (LCOE) of 0.231 \$/kWh, as presented in Table 4.1.

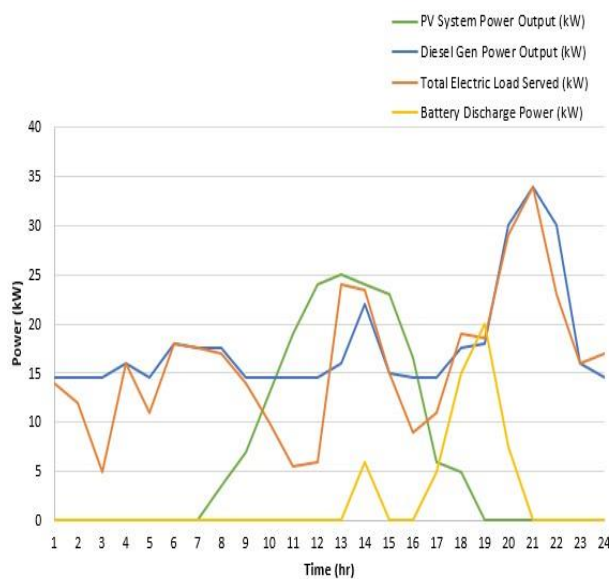


Figure 4.7a: Variation of power from PV-DG-BES & load demand for Scenario 3

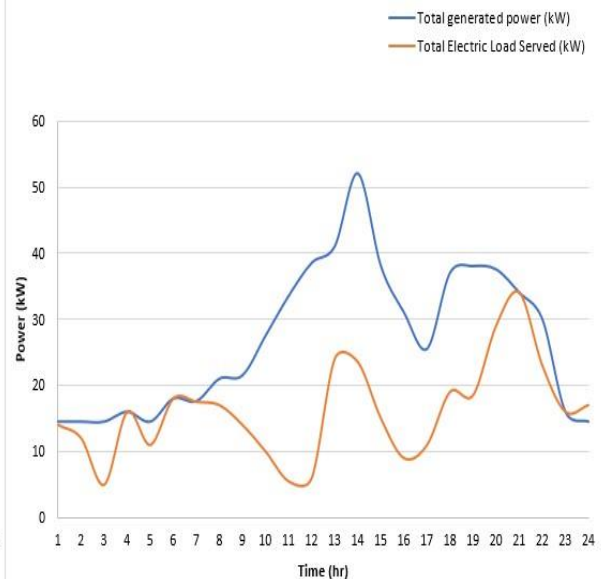


Figure 4.7b: Aggregate power from PV-DG-BES and load demand for scenario 3

Furthermore, the proposed microgrid system's reliability evaluation results were obtained by using Equations (2.1) – (2.4). The values of the LOLE and EENS results obtained are 24 hr/year and 1,600 kWh/year, respectively, as shown in Figures 4.2 and 4.3. The loss of load expectation (LOLE) value obtained in this scenario is less than the LOLE value obtained in scenario 2. This indicates that the expected hours the available generation capacity will not meet the community's power demand has reduced from 50 hrs/year to 24 hrs/year. The expected energy not served (EENS) Value in this scenario reduced more than the EENS value in scenario 2, which shows a reduction from 3,200 kWh/yr to 1,600 kWh/yr in the total energy not delivered to the load. The value of the LOLP obtained is 1.75, as shown in Figure 4.1. The probability that the daily peak will surpass the available generating capacity is lower in this scenario than in scenario 2. The cost of load loss value obtained by Equation (2.4) is 2,400 \$/yr, as shown in Figure 4.4. The cost of load loss (CLL) value obtained in this scenario is less than the CLL value obtained in scenario 2, which shows a reduction in the cost of electric outage from 5,000 \$/yr to 2,400 \$/yr owing to the reduced outage time.

4.1.4 Scenario 4

In this scenario, the diesel generator (DG) of 58 kW rating is used with 45 kW PV and 10 kW BES to meet the community's load demand. The PV-DG-BES run simultaneously to supply electrical power to the community load demand, as shown in Figure 4.8a.

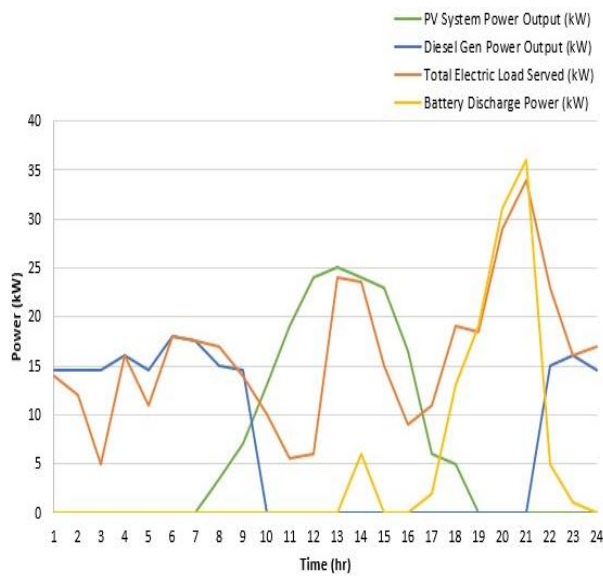


Figure 4.8a: Variation of power from PV-DG-BES & load demand for Scenario 4

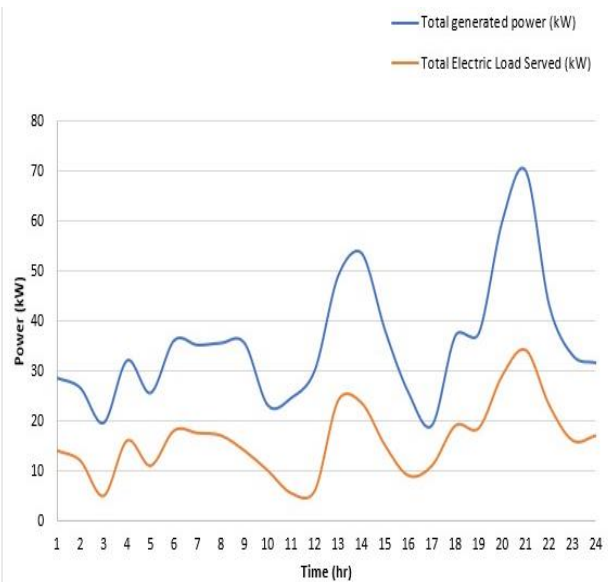


Figure 4.8b: Aggregate power from PV-DG-BES and load demand for scenario 4

It is observed that the diesel generator's operational time and output power further reduced due to the addition of further PV and BES units. 45 kW PV units and 10 kW BES units were integrated into the system in this scenario. Figure 4.8a shows that the PV system generated enough power between 9:00 to 19:00 to meet the load demand. It can be seen from Figure 4.8b that the aggregate power supplied by the PV-DG-BES met the load demand at all time.

The economic analysis result of scenario 4 presented in Table 4.1 and the reliability evaluation results obtained in Figures 4.1 to 4.4 show that the cost-saving and the system performance have significantly improved compared to scenarios 1, 2 and 3. The net present cost (NPC) of the proposed microgrid's technologies in this scenario is \$664,775 with a levelized cost of energy (LCOE) of 0.217 \$/kWh and an annual fuel cost (AFC) of 35,351 \$/year. The value of the LOLP obtained is 0.9, as shown in Figure 4.1, which shows a lower probability of outage time than in scenario 3. The LOLP value has improved compared to scenario 1, 2 and 3 due to the significant improvement in the generation capacity. The LOLE and EENS results obtained are 10 hr/year and 600 kWh/year, respectively, as shown in Figures 4.2 and 4.3.

The LOLE value obtained in this scenario shows that the expected hours the available generation capacity will not meet the community's power demand has reduced from 44 hr/year to 10 hrs/year.

The EENS value in this scenario shows a reduction in the total energy not delivered to the load from 1600 kWh/year to 600 kWh/year. The cost of load loss value in this scenario obtained using Equation (2.4) is 1000 \$/yr, as shown in Figure 4.4. The cost of load loss (CLL) value obtained in this scenario reduced from 2400 \$/yr to 1000 \$/yr, which shows that the cost of electric outage is reduced further in this scenario than in scenario 3.

4.1.5 Scenario 5

The economic and reliability evaluation was further performed to assess the effect of PV - BES in the proposed microgrid system by adding more PV and BES units into the system, as presented in Table 3.13. 60 kW PV and 15 kW BES units were incorporated into the microgrid system. The DG-PV-BES system runs simultaneously to meet the community's load demand. As shown in Figure 4.9a, the power produced by each generating unit indicates that the diesel generator's power output and operational time further reduced owing to the integration of an additional number of the PV and BES units. Figure 4.9a shows that the diesel generator supplied power between 7:00 to 10:00 in 24 hours.

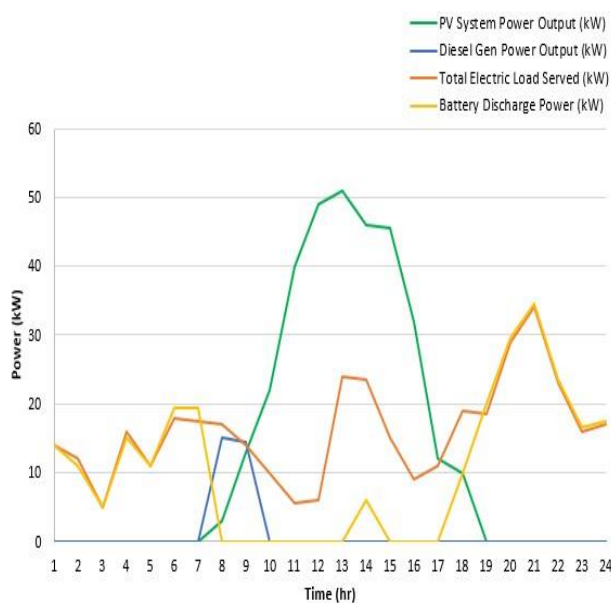


Figure 4.9a: Variation of power from PV-DG-BES & load demand for scenario 5

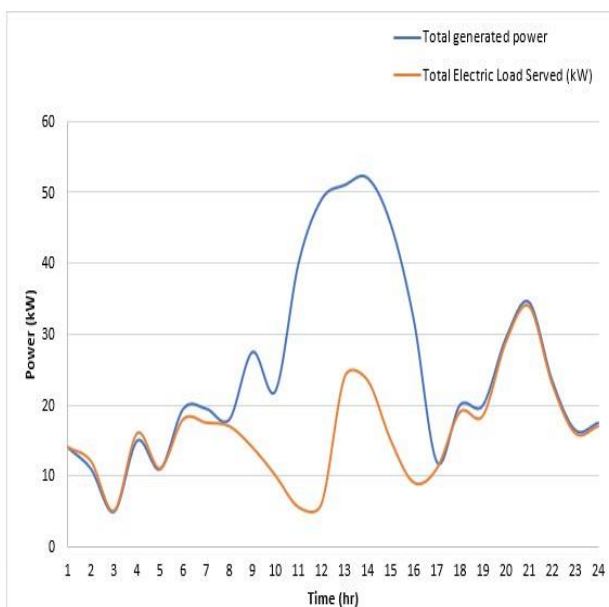


Figure 4.9b: Aggregate power from PV-DG-BES and load demand for scenario 5

The net present cost (NPC) of the proposed microgrid's technologies in this scenario is \$ 657,929 with a levelized cost of energy (LCOE) of 0.218 \$/kWh an annual fuel cost of 32,351 \$/year as presented in Table 4.1. It can be seen from Figure 4.9b that the aggregate power supplied by the PV-DG-BES met the load demand at all time. The value of the LOLP obtained is 0.9, as shown in Figure 4.1. The cost of load loss (CLL) value obtained by using Equation (2.4) is 200 \$/yr, as shown in Figure 4.4. The CLL value obtained in this scenario is less than the CLL value obtained in scenario 4, indicating a reduction in the cost of electric outage from 1000 \$/yr to 200 \$/yr due to the reduced outage time.

The LOLE and EENS results obtained are 3 hr/year and 300 kWh/year, respectively, as shown in Figures 4.2 and 4.3. The reduction in LOLE value in this scenario shows that the expected hours the available generation capacity will not meet the community's power demand has reduced from 10 hr/year to 3 hrs/year. The expected energy not served (EENS) value in this scenario reduced more than the EENS value in scenario 4, which shows a reduction from 600 kWh/yr to 100 kWh/yr in the total energy not delivered to the load.

4.1.6 Scenario 6

In this scenario, the diesel generator (DG) of 58 kW rating is used with 70 kW PV and 22 kW BES to meet the community's load demand. The PV-DG-BES run simultaneously to supply electrical power to the community load demand, as shown in Figure 4.10a.

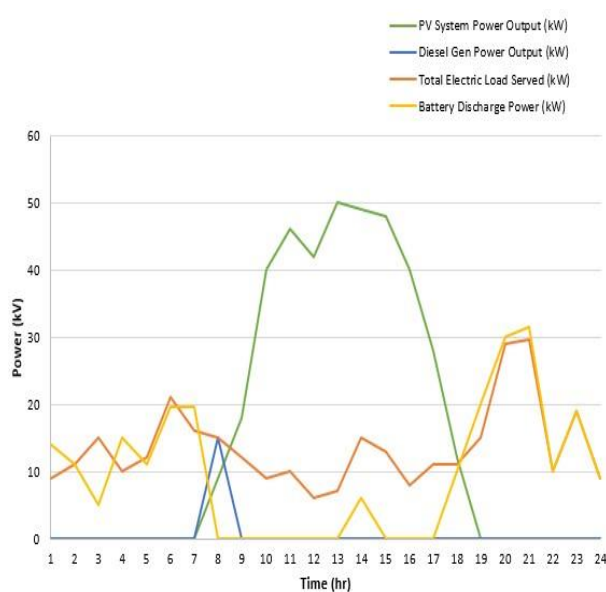


Figure 4.10a: Variation of power from PV-DG-BES & load demand for scenario 6

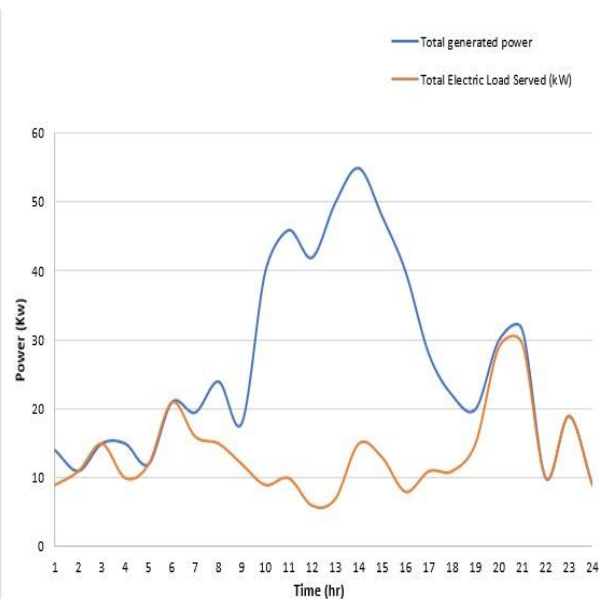


Figure 4.10b: Aggregate power from PV-DG-BES and load demand for scenario 6

Figure 4.10a shows that most of the generated power comes from the PV system, and the operation period of the diesel generator is between 7:00 to 9:00. It can be seen from Figure 4.10b that the aggregate power supplied by the PV-DG-BES met the load demand at all time. The economic evaluation result of scenario 6 presented in Table 4.1 and the reliability evaluation results obtained in Figures 4.1 to 4.4 shows that the cost-saving and the system's performance have significantly improved compared to scenarios 1-5. The net present cost (NPC) of the proposed microgrid's technologies in this scenario is \$614,191 with a levelized cost of energy (LCOE) of 0.209 \$/kWh.

The value of the LOLP obtained is less than 0, as shown in Figure 4.1, indicating that the generation capacity is sufficient to consistently meet the load demand of the community. The LOLE and EENS results obtained are 0 hr/year and 0 kWh/year, respectively, as shown in Figures 4.2 and 4.3. The LOLE value obtained in this scenario shows that the available installed capacity will consistently meet the community's power demand. The expected energy not served value shows that the generation capacity will always be enough to supply the community's energy demand. The value of cost of load loss obtained by using Equation (2.4) is 0 \$/yr, as shown in Figure 4.4, indicating that there will not be a power outage in this scenario due to a sufficient power supply.

After evaluating the 6 scenarios based on economic and reliability indicators, it is well established that scenario 6 is the most economical and reliable feasible. The economic and reliability results of scenario 6 show that the microgrid system's cost savings of the community can be enhanced by integrating 70 kW PV and 22 kW BES units to the 58 kW DG. It is also important to note that the benefits of PV-BES compared with the diesel generator depend on the solar resource availability, battery capacity, and PV unit integration level.

4.2 Sensitivity Analysis

4.2.1 Effect of PV price on LCOE

The effect of solar PV price on the LCOE of the DG-PV-BES system is shown in Figure 4.11 when the diesel fuel price is \$0.70/L, and the global solar radiation is 5.4 kWh/m²/day. As expected, a roughly linear relationship exists between the solar PV price and the LCOE. The LCOE is observed to increase by increasing PV prices of \$550/kW PV price as a base case, which is \$38,500 for the 70 kW PV capacity. With a \$550/kW PV price, the LCOE for this energy

system is estimated to decrease by about 2.9% when the PV price is reduced to \$350/kW (from \$0.209/kWh to \$0.203/kWh). However, the LCOE is observed to increase by about 4.3% (from \$0.209/kWh to \$0.218/kWh) when the PV price is increased from \$550/kW to \$850 kW. Therefore, it is concluded that the impact of PV array price on LCOE is insignificant at this location.

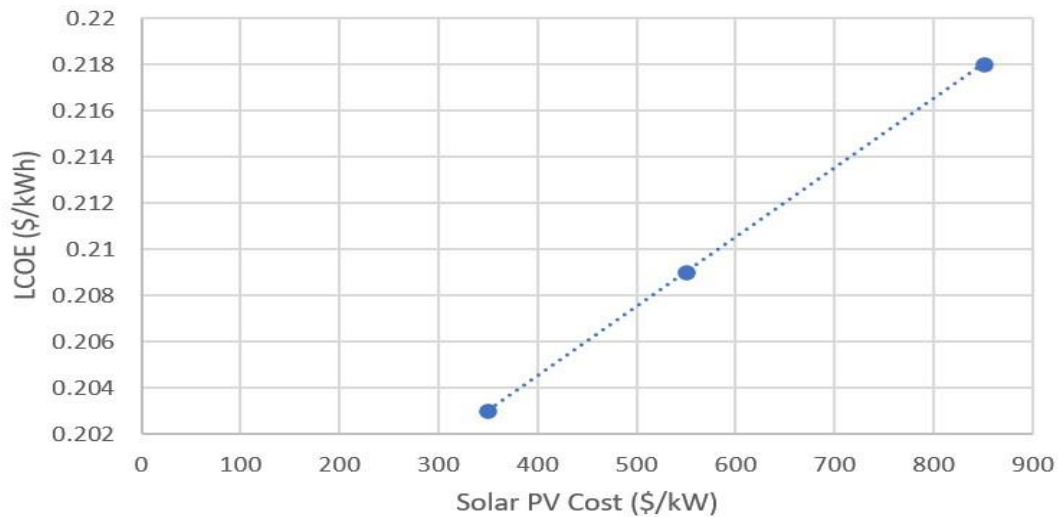


Figure 4.7: Solar PV price effect on the LCOE of the PV-DG-Battery System

4.2.2 Azimuth Angle Effect on the PV Energy Production

The PV energy production was determined for azimuth angles 0° , 90° , 180° and 270° to compare the system's performance at the location. It can be seen from Figure 4.12 that azimuth 0° yielded 103,930 kWh/yr, which produced more energy than azimuth 90° , 180° , and 270° in all the months. The annual energy yield (kWh/kWp) for azimuth 0° and 90° , 180° and 270° is presented in Table 4.2. The considered location is in the tropics and slightly above the equator. Thus, the 0° due south receives more solar irradiance than the area due east, west and north.

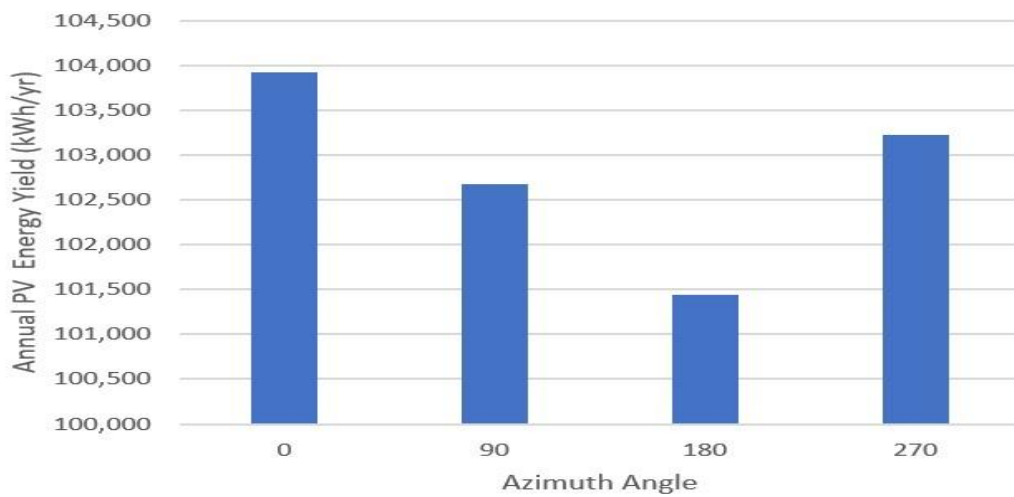


Figure 4.82: PV generated energy of Azimuth angle for 0°, 90°, 180° and 270°

Table 4.2: Installed PV System Performance

Metric	Azimuth (Y) 0° Value	Azimuth (Y) 90° Value	Azimuth (Y) 180° Value	Azimuth (Y) 270° Value
Annual Yield (kWh/kWp)	1484	1466	1449	1475
PV Capacity (kWp)	70	70	70	70

4.2.3 PV Systems Performance Based on Derating Factor

PV derating factors of 78%, 88% and 98% were considered to understand their effect on the economic and energy production on the system by applying Equation (3.14) when the diesel fuel price is \$0.70/L, and the global solar radiation is 5.4 kWh/m²/day. The annual PV energy production and the energy cost for 78%, 88% and 98% PV derating factors are shown in Table 4.3. Also, Figure 4.12 shows the techno-economic effect of the three values of the derating factor in terms of PV production and COE.

Table 4.3: Techno-Economic Performance of PV Derating Factors

PV Derating (%)	PV Lifetime (Years)	System NPC (\$)	PV Initial Capital Cost (\$)	PV Production (kWh)	System's LCOE (\$/kWh)
78	25	504,786	38,500	92,119	0.225
88	25	469,960	38,500	103,930	0.209
98	25	434,162	38,500	115,740	0.193

It can be seen from Table 4.3 and Figure 4.13 that the derating factor 98% produces more energy (115,740) than the 78% and 88% derating factor. For the derating factor of 88%, the PV panel yielded 103,930 kWh per year. The 78% derating factor produces lesser energy of 11,811 kWh than the 88% derating factor. Thus, the PV energy production is directly proportional to the derating factor.

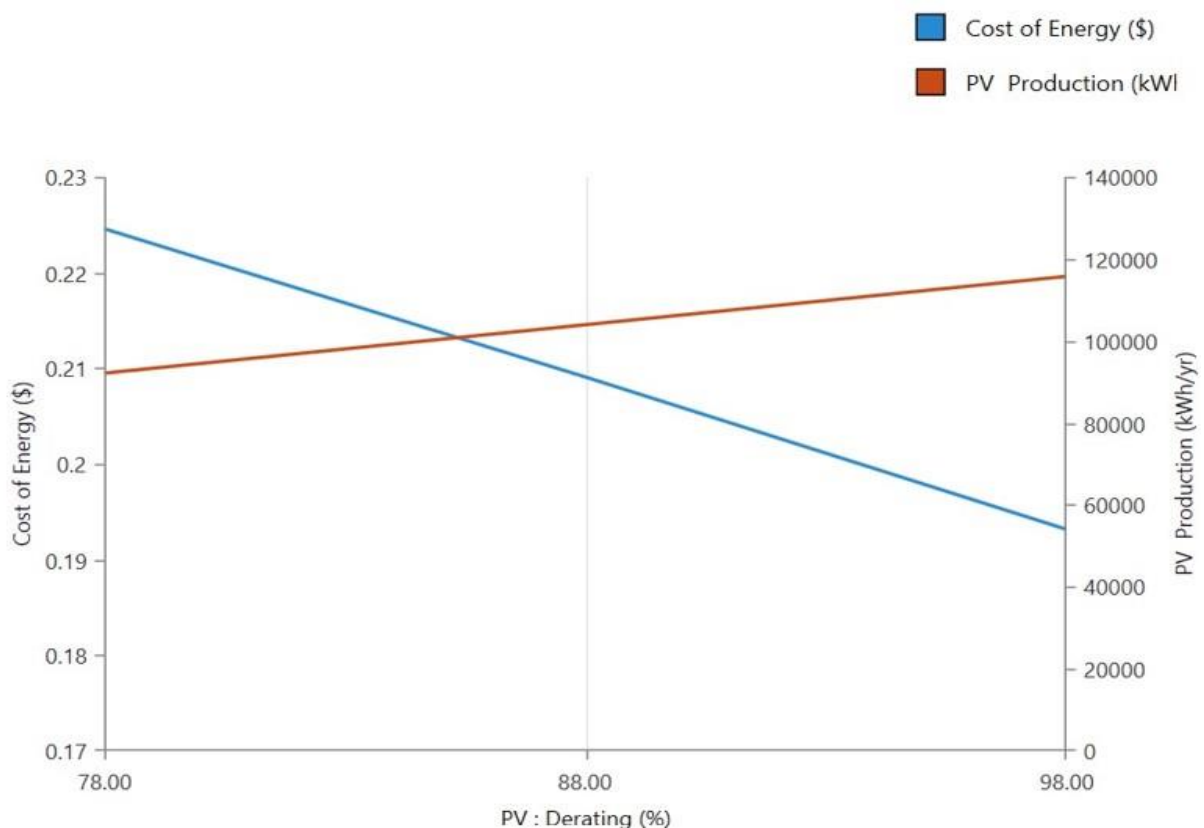


Figure 4.9: Techno-Economic Effect of the three Derating Factors

4.3 Summary

The proposed microgrid system is tested under 6 scenarios to understand better the effect of adding more PV-BES on the existing diesel generator microgrid system. From the analysis, scenario 6 provides the most cost-effective system with a LCOE of 0.31/kWh and a total NPC of \$614,191. The integration of the 70kW PV unit and 22kW BES unit in scenario 6 show how the microgrid system reliability improved with LOLP of 0, LOLE of 0h/yr, EENS of 0 kWh/yr, which is better than other scenarios. The results obtained from this study have established the significant effect of PV and BES units on the reliability and economic improvement of a microgrid system.

Chapter 5 Conclusion, Limitation and Future Work

5.0 Conclusion

This study's main objective was to evaluate the feasibility of incorporating a Photovoltaic-Battery Energy Storage System (PV-BES) into the existing Diesel Generator (DG) system to minimize the community's complete reliance on conventional energy while also improving the microgrid's reliability. The study developed a model for assessing the effects of PV-BES on a power system's reliability and economics. An economically feasible PV-BES system was proposed to solve the Ifite community's problem of the high cost of energy and frequent power outage caused by the growing energy demand. The community's existing and proposed system's reliability and economics are presented and discussed using the probability concept in MATLAB, the `fmincon` optimization tool in MATLAB, and HOMER modelling. Based on this thesis's reliability and economic analysis, utilizing PV-BES in the study area is a feasible solution for the aforementioned problem. This analysis shows that among the six scenarios for increasing the PV-BES integration level studied in this thesis, scenario 6 has the lowest levelized cost of electricity and is the most reliable. The optimization problem is based on a set of multi-objective functions that include Cost of Energy, Net Present Cost, Cost of Load Loss, and reliability analysis.

The approaches used in this research will assist power system planners and designers in assessing the economic and reliability benefits of employing PV-BES technology in Ifite community. The methods utilized in this study can be used to evaluate the effectiveness of investing in PV-BES to improve the community's generation capacity. The findings of this study reveal that the cost of energy has decreased significantly due to the use of PV-BES and improved microgrid's reliability. As a result, the most optimal option for this system is that the higher the PV-BES unit's integration level is, the more reliable and cost-effective the system becomes.

Based on that, scenario 6 gives the most cost-effective situation with LCOE of 0.209 (\$/kWh), the initial capital cost of \$192,118, NPC of \$614,191 and annual fuel costs of 24,608 (\$/year). A comparison between the existing system and the optimum scenario was conducted regarding the main three economic aspects (LCOE, AFC, NPC) and the reliability indices (LOLP,

LOLE, EENS and CLL). Scenario 6 (the best-case scenario) outperforms the existing system by lowering the LCOE from 0.255 to 0.209, nearly an 18% reduction. Furthermore, compared to the present system, the proposed system decreases the NPC from \$811,519 to \$614,191 (a 24% reduction) and the yearly fuel cost from \$55,837 to \$24,608, a 56% reduction. In terms of the reliability, the optimum scenario showed an improved reliability indices compared to the existing system as it reduces the LOLP from 2.6 to 0, LOLE from 84 hr/year to 0 hr/year, EENS from 5,800 kWh/year to 0 kWh/year and CLL from 8,500 \$/year to 0 \$/year. The following is derived from the study's findings:

- This study develops multi-objective functions that can accept a variety of inputs.
- Scenario 6 provides the best option in terms of reliability and cost.
- A microgrid system incorporating PV-BES is technically and economically better than utilizing a diesel generator solely to supply the community's power needs.
- The findings of the sensitivity analysis demonstrate that the proposed microgrid system's economic and reliability performance is dependent on:
 - Photovoltaic and battery integration level.
 - Photovoltaic and battery price changes.
 - Photovoltaic azimuthal angle variation.
 - Photovoltaic derating factor variation.

5.1 Limitation

The predicted load profile obtained for the study area was estimated using data that considered various household demographics. Another limitation of this study is that the failure rates used were obtained from the literature which has the same degradation rate and operating environment as this study's case study. Also, the study did not consider the effect of excess energy generated on the microgrid system.

5.2 Future work

This study aims to demonstrate how incorporating a PV-BES can improve the economics and reliability of a microgrid system. A future study can be conducted based on this research, considering additional issues not included in this thesis. The following are some of the aspects in the future works:

- To consider adding another suitable renewable energy like wind energy in addition to solar energy.
- To consider Fuel Cell (FC) storage system in addition to the battery storage system.
- To obtain irradiation and load profile data of one of the northern Nigerian cities due to more power outage occurrence in that part of the grid.

REFERENCES

- [1] A. Akella, R. Saini, and M. P. J. R. E. Sharma, "Social, economical and environmental impacts of renewable energy systems," *Renewable Energy*, vol. 34, no. 2, pp. 390-396, 2009.
- [2] C. O. Okoye, O. Taylan, D. K. J. R. Baker, and S. E. Reviews, "Solar energy potentials in strategically located cities in Nigeria: Review, resource assessment and PV system design," *Renewable and Sustainable Energy Reviews*, vol. 55, pp. 550-566, 2016.
- [3] O. C. Egbon, "Optimal Sizing of a Standalone Photovoltaic (PV) System for Residential Customers Considering Electricity Consumption Patterns: A Case Study of Ibadan City, Nigeria," *PhD diss.*, Auckland University of Technology, 2019.
- [4] E. J. T. E. J. Adhekpukoli, "The democratization of electricity in Nigeria," *The Electricity Journal*, vol. 31, no. 2, pp. 1-6, 2018.
- [5] S. O. J. E. Oyedepo, Sustainability and Society, "Energy and sustainable development in Nigeria: the way forward," *Energy, Sustainability and Society*, vol. 2, no. 1, p. 15, 2012.
- [6] T. Kemabonta and M. Kabalan, "Using What You Have, to Get What You Want—A Different Approach to Electricity Market Design for Local Distribution Companies (DISCOs) in Nigeria," in *2018 IEEE Global Humanitarian Technology Conference (GHTC)*, 2018, pp. 1-2: IEEE.
- [7] M. Shaaban, J. J. R. Petinrin, and S. E. Reviews, "Renewable energy potentials in Nigeria: Meeting rural energy needs," *Renewable and sustainable energy reviews*, vol. 29, pp. 72-84, 2014.
- [8] E. I. Administration and E. Department, *Annual energy outlook 2015: With projections to 2040*. Government Printing Office, *Energy Policy*, vol. 109 pp. 279-287, 2015.
- [9] Y. Mekonnen and A. I. Sarwat, "Renewable energy supported microgrid in rural electrification of Sub-Saharan Africa," in *2017 IEEE PES PowerAfrica*, 2017, pp. 595-599: IEEE.
- [10] J. J. Popoola, A. A. Ponnle, and T. O. J. A. J. Ale, "Reliability worth assessment of electric power utility in Nigeria: Residential customer survey results," *AUJT*, vol. 14, no. 3, pp. 217-224, 2011.
- [11] H. N. J. J. o. E. T. Amadi and Policy, "Impact of power outages on developing countries: evidence from rural households in Niger Delta, Nigeria," *Journal of Energy Technologies and Policy*, vol. 5, no. 3, pp. 27-38, 2015.
- [12] C. Egbon, A. Oyekola, and T.-T. Lie, "Design of stand alone photovoltaic system in developing countries: A case study of Kano, Nigeria," in *2018 Australasian Universities Power Engineering Conference (AUPEC)*, 2018, pp. 1-6: IEEE.
- [13] M. Rausand and A. Hoyland, *System reliability theory: models, statistical methods, and applications*. John Wiley & Sons, 2003.
- [14] S. Babu, P. Hilber, and J. H. Jürgensen, "On the status of reliability studies involving primary and secondary equipment applied to power system," in *2014 International Conference on Probabilistic Methods Applied to Power Systems (PMAPS)*, 2014, pp. 1-6: IEEE.
- [15] N. E. R. Commission, "Regulations on Feed-in Tariff for Renewable Energy Sourced Electricity in Nigeria. *The Electricity Journal*, 2015," ed.
- [16] N. Balijepalli, S. S. Venkata, and R. D. J. I. T. o. P. D. Christie, "Modeling and analysis of distribution reliability indices," *IEEE Transactions on Power Delivery*, vol. 19, no. 4, pp. 1950-1955, 2004.
- [17] W. Li, L. Sun, W. Zou, and C. Luo, "Power system reliability analysis system based on PSASP and fault enumeration method and applications," in *2014 China International Conference on Electricity Distribution (CICED)*, 2014, pp. 1323-1326: IEEE.
- [18] W. Peng, H.-Z. Huang, M. Xie, Y. Yang, and Y. J. I. T. o. R. Liu, "A Bayesian approach for system reliability analysis with multilevel pass-fail, lifetime and degradation data sets," *IEEE Transactions on Reliability*, vol. 62, no. 3, pp. 689-699, 2013.
- [19] Y. Xiang, L. Wang, and T. Fu, "A preliminary study of power system reliability considering cloud service reliability," in *2014 International Conference on Power System Technology*, 2014, pp. 2031-2036: IEEE.

- [20] W. Li, *Reliability assessment of electric power systems using Monte Carlo methods*. Springer Science & Business Media, 2013.
- [21] R. Billinton, R. N. J. E. Allan, and Power, "Power-system reliability in perspective," *Electronics and Power*, vol. 30, no. 3, pp. 231-236, 1984.
- [22] M. Zima, "Contributions to security of electric power systems," PhD diss., ETH Zurich, 2006.
- [23] R. N. Allan, *Reliability evaluation of power systems*. Springer Science & Business Media, 2013.
- [24] W. J. I. T. o. P. s. Li, "Incorporating aging failures in power system reliability evaluation," *IEEE Transactions on Power systems*, vol. 17, no. 3, pp. 918-923, 2002.
- [25] R. Billinton, M. Fotuhi-Firuzabad, and L. J. I. T. o. P. S. Bertling, "Bibliography on the application of probability methods in power system reliability evaluation 1996-1999," *IEEE Transactions on Power systems*, vol. 16, no. 4, pp. 595-602, 2001.
- [26] S. K. Khator and L. C. J. I. T. o. P. S. Leung, "Power distribution planning: A review of models and issues," *IEEE Transactions on Power systems*, vol. 12, no. 3, pp. 1151-1159, 1997.
- [27] M. M. Ghahderijani, S. M. Barakati, and S. Tavakoli, "Reliability evaluation of stand-alone hybrid microgrid using Sequential Monte Carlo Simulation," in *2012 Second Iranian Conference on Renewable Energy and Distributed Generation*, 2012, pp. 33-38: IEEE.
- [28] R. J. I. T. o. P. S. Billinton, "Criteria used by Canadian utilities in the planning and operation of generating capacity," *IEEE Transactions on Power systems*, vol. 3, no. 4, pp. 1488-1493, 1988.
- [29] J. F. Prada, "The value of reliability in power systems-pricing operating reserves," 1999.
- [30] M. Shirvani, A. Memaripour, M. Abdollahi, and A. J. L. s. j. Salimi, "Calculation of generation system reliability index: Expected Energy Not Served," *Life science journal*, vol. 9, no. 4, pp. 3443-3448, 2012.
- [31] T. Adefarati and R. C. J. A. e. Bansal, "Reliability, economic and environmental analysis of a microgrid system in the presence of renewable energy resources," *Applied energy*, vol. 236, pp. 1089-1114, 2019.
- [32] J. J. Nelson, G. Venkataramanan, and A. M. J. I. T. o. i. E. El-Refaie, "Fast thermal profiling of power semiconductor devices using Fourier techniques," *IEEE Transactions on industrial Electronics*, vol. 53, no. 2, pp. 521-529, 2006.
- [33] W. Sarjeant, F. MacDougall, D. Larson, and I. J. I. T. o. M. Kohlberg, "Energy storage capacitors: aging, and diagnostic approaches for life validation," *IEEE Transactions on Magnetics*, vol. 33, no. 1, pp. 501-506, 1997.
- [34] T. Adefarati, R. C. Bansal, and J. J. E. P. Justo, "Reliability and economic evaluation of a microgrid power system," *Energy Procedia*, vol. 142, pp. 43-48, 2017.
- [35] A. B. Esan, A. F. Agbetuyi, O. Oghorada, K. Ogbeide, A. A. Awelewa, and A. E. J. H. Afolabi, "Reliability assessments of an islanded hybrid PV-diesel-battery system for a typical rural community in Nigeria," *Heliyon*, vol. 5, no. 5, p. e01632, 2019.
- [36] M. Papadrakakis, N. D. J. C. m. i. a. m. Lagaros, and engineering, "Reliability-based structural optimization using neural networks and Monte Carlo simulation," *Computer methods in applied mechanics and engineering*, vol. 191, no. 32, pp. 3491-3507, 2002.
- [37] H. Liang, J. Su, and S. Liu, "Reliability evaluation of distribution system containing microgrid," in *CICED 2010 Proceedings*, 2010, pp. 1-7: IEEE.
- [38] H. F. Boroujeni, M. Eghtedari, M. Abdollahi, and E. J. L. S. J. Behzadipour, "Calculation of generation system reliability index: Loss of Load Probability," *Life Science Journal*, vol. 9, no. 4, pp. 4903-4908, 2012.
- [39] T. Vrana and E. J. C. Johansson, "Overview of power system reliability assessment techniques," *Applied energy*, pp. 51-62, 2011.
- [40] P. Zhang, W. Li, S. Li, Y. Wang, and W. J. A. e. Xiao, "Reliability assessment of photovoltaic power systems: Review of current status and future perspectives," *Applied energy*, vol. 104, pp. 822-833, 2013.

- [41] R. Dufo-López *et al.*, "Multi-objective optimization minimizing cost and life cycle emissions of stand-alone PV–wind–diesel systems with batteries storage," *Applied Energy*, vol. 88, no. 11, pp. 4033-4041, 2011.
- [42] A. Al-Karaghoul and L. J. S. E. Kazmerski, "Optimization and life-cycle cost of health clinic PV system for a rural area in southern Iraq using HOMER software," *Solar Energy*, vol. 84, no. 4, pp. 710-714, 2010.
- [43] V. A. J. F. i. E. R. Ani, "Design of a stand-alone photovoltaic model for home lightings and clean environment," *Frontiers in Energy Research*, vol. 3, p. 54, 2016.
- [44] A. K. Shukla, K. Sudhakar, and P. J. S. E. Baredar, "Design, simulation and economic analysis of standalone roof top solar PV system in India," *Solar Energy*, vol. 136, pp. 437-449, 2016.
- [45] N. Mukisa, R. Zamora, T. T. J. S. E. T. Lie, and Assessments, "Feasibility assessment of grid-tied rooftop solar photovoltaic systems for industrial sector application in Uganda," *Sustainable Energy Technologies and Assessments*, vol. 32, pp. 83-91, 2019.
- [46] T. Givler and P. Lilienthal, "Using HOMER Software, NREL's Micropower Optimization Model, to Explore the Role of Gen-sets in Small Solar Power Systems; Case Study: Sri Lanka," National Renewable Energy Lab., Golden, CO (US)2005.
- [47] S. Salisu, M. W. Mustafa, L. Olatomiwa, and O. O. J. A. E. J. Mohammed, "Assessment of technical and economic feasibility for a hybrid PV-wind-diesel-battery energy system in a remote community of north central Nigeria," *Alexandria Engineering Journal*, vol. 58, no. 4, pp. 1103-1118, 2019.
- [48] A. Limmanee *et al.*, "Degradation analysis of photovoltaic modules under tropical climatic conditions and its impacts on LCOE," *Renewable energy*, vol. 102, pp. 199-204, 2017.
- [49] A. M. Al-Shaalan, "Reliability evaluation of power systems," in *Reliability and Maintenance-An Overview of Cases*: IntechOpen, 2019.
- [50] F. J. Ardakani, G. Riahy, and M. Abedi, "Design of an optimum hybrid renewable energy system considering reliability indices," in *2010 18th Iranian conference on electrical engineering*, 2010, pp. 842-847: IEEE.
- [51] A. Sinha, "A Power System Reliability Evaluation Technique and Education Tool for Wind Energy Integration," *PhD diss.*, Arizona State University, 2012.
- [52] M. O. M. Mahmoud, M. Jaidane-Saidane, J. Souissi, and N. Hizaoui, "Modeling of the load duration curve using the asymmetric generalized Gaussian distribution: Case of the Tunisian power system," in *2008 IEEE Power and Energy Society General Meeting-Conversion and Delivery of Electrical Energy in the 21st Century*, 2008, pp. 1-7: IEEE.
- [53] A. Ghafoor, A. J. R. Munir, and S. E. Reviews, "Design and economics analysis of an off-grid PV system for household electrification," *Renewable and Sustainable Energy Reviews*, vol. 42, pp. 496-502, 2015.
- [54] N. D. Nordin and H. A. Rahman, "Design and economic analysis in stand alone photovoltaic system," in *2014 IEEE Conference on Energy Conversion (CENCON)*, 2014, pp. 152-157: IEEE.
- [55] L. Ciabattoni, M. Grisostomi, G. Ippoliti, and S. J. E. Longhi, "Fuzzy logic home energy consumption modeling for residential photovoltaic plant sizing in the new Italian scenario," *Energy*, vol. 74, pp. 359-367, 2014.
- [56] I. Ibrik and M. Lecumberri, "Techno-economic feasibility of energy supply of remote villages in Palestine by PV-systems, diesel generators and electric grid (Case studies: Emnazeil and Atouf villages)," 2010.
- [57] T. Lambert, P. Gilman, and P. J. I. o. a. s. o. e. Lilienthal, "Micropower system modeling with HOMER," *Integration of alternative sources of energy*, vol. 1, no. 1, pp. 379-385, 2006.
- [58] U. Manandhar, A. Ukil, and T. K. K. Jonathan, "Efficiency comparison of DC and AC microgrid," in *2015 IEEE Innovative Smart Grid Technologies-Asia (ISGT ASIA)*, 2015, pp. 1-6: IEEE.
- [59] O. S. Idowu, O. M. Olarenwaju, O. I. J. I. J. o. E. Ifedayo, and E. Engineering, "Determination of optimum tilt angles for solar collectors in low-latitude tropical region," *International Journal of Energy and Environmental Engineering*, vol. 4, no. 1, pp. 1-10, 2013.

- [60] A. N. Al-Shamani *et al.*, "Design & sizing of stand-alone solar power systems a house Iraq," pp. 145-150, 2015.
- [61] H. A. Attia, B. N. Getu, N. A. J. I. J. o. T. Hamad, and E. Engineering, "A Stable DC Power Supply for Photovoltaic Systems," *Int. J. of Thermal & Environmental Engineering*, vol. 12, no. 1, pp. 67-71, 2016.
- [62] *GENERATOR SET ISO 8528 POWER RATINGS EXPLAINED*. Available: <http://www.fgwilson.ie/files/generator-set-iso-8528-power-ratings-explained.pdf>
- [63] T. Adefarati, N. B. Papy, M. Thopil, and H. J. H. o. D. G. Tazvinga, "Non-renewable distributed generation technologies: A review," *Handbook of distributed generation*, pp. 69-105, 2017.
- [64] J. D. Navamani, A. Lavanya, C. Prahadheeshwar, and S. M. J. I. J. R. T. E. Riyazudeen, "Hybrid power system design using Homer Pro," *Int. J. Recent Technol. Eng*, vol. 8, p. 4, 2019.
- [65] G. Aghajani, H. Shayanfar, and H. J. E. Shayeghi, "Demand side management in a smart micro-grid in the presence of renewable generation and demand response," *Energy*, vol. 126, pp. 622-637, 2017.
- [66] "SMA, "SC500HE grid tied inverter 3-Phase 500kW."
- [67] *HOMER Pro User Manual*. Homer Energy, Boulder, CO, USA. Available: <https://www.homerenergy.com/products/pro/docs/latest/index.html>
- [68] B. K. Das, Y. M. Al-Abdeli, and G. J. A. e. Kothapalli, "Optimisation of stand-alone hybrid energy systems supplemented by combustion-based prime movers," *Applied energy*, vol. 196, pp. 18-33, 2017.

Appendices

APPENDIX A: MATLAB Codes for the COPT Calculation

```

% This is a function file: GeneratorCOPT(G,PR,A)
% This calculates the 'Outage Probability' for a single Power
SGeneratorCOPTMatrixion
% G stands for number of generating unit
% PR stands for Power Ratings of each unit (in Array form)
% A stands for Availability of each unit (in Array form)

function Generator_COPT(G,PR,A);
G=1;
PR=[65];
A=[0.04];
format short g
X=ff2n(G);
InitiationMatrix=[zeros(1,2^G);zeros(1,2^G);ones(1,2^G);zeros(1,2^G)];
GeneratorCOPTMatrixTemp=InitiationMatrix';
for j=1:2^G
for i=1:G
    if (X(j,i)==0)
        GeneratorCOPTMatrixTemp(j,1)=GeneratorCOPTMatrixTemp(j,1)+PR(i,1);
        GeneratorCOPTMatrixTemp(j,3)=GeneratorCOPTMatrixTemp(j,3)*A(i,1);
    else
        GeneratorCOPTMatrixTemp(j,2)=GeneratorCOPTMatrixTemp(j,2)+PR(i,1);
        GeneratorCOPTMatrixTemp(j,3)=GeneratorCOPTMatrixTemp(j,3)*(1-
A(i,1));
    end
end
end
TemporaryMatrix=GeneratorCOPTMatrixTemp;
for m=1:(2^G)
    for n=1:(2^G)
        if (GeneratorCOPTMatrixTemp(m,1)==GeneratorCOPTMatrixTemp(n,1) && m~=n &&
n>m)

GeneratorCOPTMatrixTemp(m,3)=GeneratorCOPTMatrixTemp(m,3)+GeneratorCOPTMatr
ixTemp(n,3);
        else end
    end
end
for m=1:2^G
    for n=1:2^G
        if (GeneratorCOPTMatrixTemp(m,1)==GeneratorCOPTMatrixTemp(n,1) &&
m<n && m~=n && GeneratorCOPTMatrixTemp(m,1)~=0)
            GeneratorCOPTMatrixTemp(n,:)=zeros;
        else end
    end
end
for m=1:1:(2^G)-1
    for n=1:1:(2^G)-1
        if (GeneratorCOPTMatrixTemp(n,1)<GeneratorCOPTMatrixTemp((n+1),1))
            temp1=GeneratorCOPTMatrixTemp(n,1);
            temp2=GeneratorCOPTMatrixTemp(n,2);
            temp3=GeneratorCOPTMatrixTemp(n,3);
            GeneratorCOPTMatrixTemp(n,1)=GeneratorCOPTMatrixTemp((n+1),1);
            GeneratorCOPTMatrixTemp(n,2)=GeneratorCOPTMatrixTemp((n+1),2);
            GeneratorCOPTMatrixTemp(n,3)=GeneratorCOPTMatrixTemp((n+1),3);
        end
    end
end

```


APPENDIX B: MATLAB code for the LOLP, CLL, EENS and LOLE calculation

(Top Run Design)

```

clc
clear all
close all

%%
DIFFERENT_CASE_DATA=[
    1 58 0 0
    1 58 0 0
    2 58 10 0
    3 58 15 4
    4 58 20 6
    5 58 25 8
    6 58 70 22
];
FORCED_OUTAGE_RATE=[0.06 0.03 0.03];
data=xlsread('Final_pvwatts_hourly.csv');
daily_load_inform=data(16:end-1,end);
daily_load_inforf=reshape(daily_load_inform,[24 365]);
daily_load_inform=max(daily_load_inforf);
loadcurv=sort(daily_load_inform,'descend');
peakload=max(loadcurv);
% OPTIONS = optimoptions(SOLVER) creates optimization options, OPTIONS,
% with the option parameters set to the default values relevant to the
% optimization solver named in SOLVER, for example 'fmincon'.

algorith_option=optimoptions('fmincon','Algorithm','interior-point');
algorith_option.Display='iter';
% algorith_option.TolX = 0.01;
% algorith_option.MaxIter = 1000;

rangemax=100;

%% scenario 1
casedata=DIFFERENT_CASE_DATA(2,2:end)*rangemax;
casedatami=DIFFERENT_CASE_DATA(1,2:end);
% set maximum limit
pmax_diesel=casedata(1);pmax_pv=casedata(2);
pmax_ess=casedata(3);
% set minimum limit
pmin_diesel=casedatami(1);pmin_pv=casedatami(2);
pmin_ess=casedatami(3);
% set upper and lower limit
lowerlmt=[pmin_diesel pmin_pv pmin_ess];
upperlmt=[pmax_diesel pmax_pv pmax_ess];
final_demand_load=peakload;
num=length(casedata);
initialdata=lowerlmt+(upperlmt-lowerlmt).*rand(1,num);
% set constraints
eq_constraint=[1 1 1]; eq_constr_data=[final_demand_load];
uneq_ctr=[];uneq_ctr_data=[];
% fmincon finds a constrained minimum of a function of several variables.
% fmincon attempts to solve problems of the form:
% min F(X) subject to: A*X <= B, Aeq*X = Beq (linear constraints)
% X C(X) <= 0, Ceq(X) = 0 (nonlinear constraints)
% LB <= X <= UB (bounds)

```

```

fminconresdata=fmincon(@(datain)objective_process(datain,loadcurv,num,FORCE
D_OUTAGE_RATE),initialdata,...

uneq_ctr,uneq_ctr_data,eq_constraint,eq_constr_data,lowerlmt,upperlmt,[],al
gorithm_option);
% call objective process to find best
[~,resf]=objective_process(fminconresdata,loadcurv,num,FORCED_OUTAGE_RATE);
final_result_data(:,1)=(resf. ');
finalfimd=fminconresdata(1);
finaloutpower1=fminconresdata;

%% scenario 2
casedata=DIFFERENT_CASE_DATA(3,2:end)*rangemax;
casedatami=DIFFERENT_CASE_DATA(2,2:end);
% set maximum limit
pmax_diesel=casedata(1);pmax_pv=casedata(2);
pmax_ess=casedata(3);
% set minimum limit
pmin_diesel=casedatami(1);pmin_pv=casedatami(2);
pmin_ess=casedatami(3);
lowerlmt=[pmin_diesel pmin_pv pmin_ess];
upperlmt=[pmax_diesel pmax_pv pmax_ess];
final_demand_load=peakload;
num=length(casedata);
initialdata=lowerlmt+(upperlmt-lowerlmt).*rand(1,num);
% set constraints
eq_constraint=[1 1 1]; eq_constr_data=[final_demand_load];
uneq_ctr=[];uneq_ctr_data=[];
% fmincon finds a constrained minimum of a function of several variables.
% fmincon attempts to solve problems of the form:
% min F(X) subject to: A*X <= B, Aeq*X = Beq (linear constraints)
% X C(X) <= 0, Ceq(X) = 0 (nonlinear constraints)
% LB <= X <= UB (bounds)

fminconresdata=fmincon(@(datain)objective_process(datain,loadcurv,num,FORCE
D_OUTAGE_RATE),initialdata,...

uneq_ctr,uneq_ctr_data,eq_constraint,eq_constr_data,lowerlmt,upperlmt,[],al
gorithm_option);
% call objective process to find best
[~,resf]=objective_process(fminconresdata,loadcurv,num,FORCED_OUTAGE_RATE);
final_result_data(:,2)=(resf. ');
fminconresdata(1)=finalfimd;
finaloutpower2=fminconresdata;

%% scenario 3
casedata=DIFFERENT_CASE_DATA(4,2:end)*rangemax;
casedatami=DIFFERENT_CASE_DATA(3,2:end);

% set maximum limit
pmax_diesel=casedata(1);pmax_pv=casedata(2);
pmax_ess=casedata(3);
% set minimum limit
pmin_diesel=casedatami(1);pmin_pv=casedatami(2);
pmin_ess=casedatami(3);
upperlmt=[pmax_diesel pmax_pv pmax_ess];
final_demand_load=peakload;
num=length(casedata);
initialdata=lowerlmt+(upperlmt-lowerlmt).*rand(1,num);
% set constraints
eq_constraint=[1 1 1]; eq_constr_data=[final_demand_load];

```

```

uneq_ctr=[];uneq_ctr_data=[];
% fmincon finds a constrained minimum of a function of several variables.
% fmincon attempts to solve problems of the form:
% min F(X) subject to: A*X <= B, Aeq*X = Beq (linear constraints)
% X C(X) <= 0, Ceq(X) = 0 (nonlinear constraints)
% LB <= X <= UB (bounds)

fminconresdata=fmincon(@(datain)objective_process(datain,loadcurv,num,FORCE
D_OUTAGE_RATE),initialdata,...

uneq_ctr,uneq_ctr_data,eq_constraint,eq_constr_data,lowerlmt,upperlmt,[],al
gorithm_option);
% call objective process to find best
[~,resf]=objective_process(fminconresdata,loadcurv,num,FORCED_OUTAGE_RATE);
final_result_data(:,3)=(resf. ');
fminconresdata(1)=finalfimd;
finaloutpower3=fminconresdata;

%% scenario 4
casedata=DIFFERENT_CASE_DATA(5,2:end)*rangemax;
casedatami=DIFFERENT_CASE_DATA(4,2:end);
% set maximum limit
pmax_diesel=casedata(1);pmax_pv=casedata(2);
pmax_ess=casedata(3);
% set minimum limit
pmin_diesel=casedatami(1);pmin_pv=casedatami(2);
pmin_ess=casedatami(3);
lowerlmt=[pmin_diesel pmin_pv pmin_ess];
upperlmt=[pmax_diesel pmax_pv pmax_ess];
final_demand_load=peakload;
num=length(casedata);
initialdata=lowerlmt+(upperlmt-lowerlmt).*rand(1,num);
% set constraints
eq_constraint=[1 1 1]; eq_constr_data=[final_demand_load];
uneq_ctr=[];uneq_ctr_data=[];
% fmincon finds a constrained minimum of a function of several variables.
% fmincon attempts to solve problems of the form:
% min F(X) subject to: A*X <= B, Aeq*X = Beq (linear constraints)
% X C(X) <= 0, Ceq(X) = 0 (nonlinear constraints)
% LB <= X <= UB (bounds)

fminconresdata=fmincon(@(datain)objective_process(datain,loadcurv,num,FORCE
D_OUTAGE_RATE),initialdata,...

uneq_ctr,uneq_ctr_data,eq_constraint,eq_constr_data,lowerlmt,upperlmt,[],al
gorithm_option);
% call objective process to find best
[~,resf]=objective_process(fminconresdata,loadcurv,num,FORCED_OUTAGE_RATE);
final_result_data(:,4)=(resf. ');
fminconresdata(1)=finalfimd;
finaloutpower4=fminconresdata;

%% scenario 5
casedata=DIFFERENT_CASE_DATA(6,2:end)*rangemax;
casedatami=DIFFERENT_CASE_DATA(5,2:end);
% set maximum limit
pmax_diesel=casedata(1);pmax_pv=casedata(2);
pmax_ess=casedata(3);
% set minimum limit
pmin_diesel=casedatami(1);pmin_pv=casedatami(2);
pmin_ess=casedatami(3);
lowerlmt=[pmin_diesel pmin_pv pmin_ess];

```

```

upperlmt=[pmax_diesel pmax_pv pmax_ess];
final_demand_load=peakload;
num=length(casedata);
initialdata=lowerlmt+(upperlmt-lowerlmt).*rand(1,num);
% set constraints
eq_constraint=[1 1 1]; eq_constr_data=[final_demand_load];
uneq_ctr=[];uneq_ctr_data=[];
% fmincon finds a constrained minimum of a function of several variables.
% fmincon attempts to solve problems of the form:
% min F(X) subject to: A*X <= B, Aeq*X = Beq (linear constraints)
% X C(X) <= 0, Ceq(X) = 0 (nonlinear constraints)
% LB <= X <= UB (bounds)

fminconresdata=fmincon(@(datain) objective_process (datain,loadcurv,num,FORCE
D_OUTAGE_RATE),initialdata,...

uneq_ctr,uneq_ctr_data,eq_constraint,eq_constr_data,lowerlmt,upperlmt,[],al
gorithm_option);
% call objective process to find best
[~,resf]=objective_process (fminconresdata,loadcurv,num,FORCED_OUTAGE_RATE);
final_result_data(:,5)=(resf. ');
fminconresdata(1)=finalfimd;
finaloutpower5=fminconresdata;

%% scenario 6
casedata=DIFFERENT_CASE_DATA(7,2:end)*rangemax;
casedatami=DIFFERENT_CASE_DATA(6,2:end);
% set maximum limit
pmax_diesel=casedata(1);pmax_pv=casedata(2);
pmax_ess=casedata(3);
% set minimum limit
pmin_diesel=casedatami(1);pmin_pv=casedatami(2);
pmin_ess=casedatami(3);
lowerlmt=[pmin_diesel pmin_pv pmin_ess];
upperlmt=[pmax_diesel pmax_pv pmax_ess];
final_demand_load=peakload;
num=length(casedata);
initialdata=lowerlmt+(upperlmt-lowerlmt).*rand(1,num);
% set constraints
eq_constraint=[1 1 1]; eq_constr_data=[final_demand_load];
uneq_ctr=[];uneq_ctr_data=[];
% fmincon finds a constrained minimum of a function of several variables.
% fmincon attempts to solve problems of the form:
% min F(X) subject to: A*X <= B, Aeq*X = Beq (linear constraints)
% X C(X) <= 0, Ceq(X) = 0 (nonlinear constraints)
% LB <= X <= UB (bounds)

fminconresdata=fmincon(@(datain) objective_process (datain,loadcurv,num,FORCE
D_OUTAGE_RATE),initialdata,...

uneq_ctr,uneq_ctr_data,eq_constraint,eq_constr_data,lowerlmt,upperlmt,[],al
gorithm_option);
% call objective process to find best
[~,resf]=objective_process (fminconresdata,loadcurv,num,FORCED_OUTAGE_RATE);
final_result_data(:,6)=(resf. ');
fminconresdata(1)=finalfimd;
finaloutpower6=fminconresdata;
%%
finaloutpower=[finaloutpower1 ;finaloutpower2 ;finaloutpower3;
finaloutpower4;finaloutpower5;finaloutpower6]/1.3;
AMC=num2str(final_result_data(1,:). ');
AFC=num2str(final_result_data(2,:). ');

```

```

%AEC=num2str(final_result_data(3,:).');
%ACC=num2str(final_result_data(4,:).');
%ARC=num2str(final_result_data(4,:).');
ACS=num2str(final_result_data(5,:).');
NPC=num2str(final_result_data(4,:).');
COE=num2str(final_result_data(6,:).');

SCENARIO={'1','2','3','4','5','6'}.';
RESULT=table(SCENARIO,AFC,NPC,COE)
%%
%daily_load_inform=max(daily_load_inforf);
%loadcurv=sort(daily_load_inform,'descend');
%peakload=max(loadcurv);
%figure,plot(daily_load_inform,'b-o','linewidth',2);
%title('Daily peak load');
%grid on;xlabel('day');ylabel('Demand kW');

%figure,plot(loadcurv,'b-o','linewidth',2);
%title('Daily Peak Load Variation Curve');
%grid on;xlabel('day');ylabel('Demand kW');

FORCED_OUTAGE_RATE=[0.06 0.03 0.03];
looploc=1;
for indl=1:6
    genunit=finaloutpower(indl,:);
    number_of_unit=length(genunit);
    uint_power_generate=[rot90(cumsum(genunit),2) 0];
    uint_power_generate=cumsum(uint_power_generate);

prop_unavail=ones(1,number_of_unit).*FORCED_OUTAGE_RATE(1:number_of_unit);
prop_avail=1-prop_unavail;
peakload=max(loadcurv);

indival_prop_system=prop_of_system(prop_avail,prop_unavail,number_of_unit);

    for km=1:length(uint_power_generate)
        chk_lmt_exceed=find(loadcurv>uint_power_generate(km));
        totaltime=length(chk_lmt_exceed);

final_lole(km)=indival_prop_system(km)*sum(loadcurv(chk_lmt_exceed)-
uint_power_generate(km));
        final_lolp(km)=totaltime*indival_prop_system(km);
        final_ens(km)=sum(loadcurv(chk_lmt_exceed)-
uint_power_generate(km));
    end

    LOLP(looploc)=sum(final_lolp);
    LOLE(looploc)=sum(final_lole)/60;
    EENS(looploc)=sum(final_ens);
    COST_OF_LOAD_LOSS(looploc)=sum(final_ens)*1.5;
    looploc=looploc+1;

end
figure,plot(1:6,LOLP,'r-s','linewidth',2);
xlabel('SCENARIOS');ylabel('LOLP');grid on;
namelg=SCENARIO;
set(gca,'XTick',1:6,'XTickLabel',namelg);

figure,plot(1:6,LOLE,'r-s','linewidth',2);

```

```
xlabel('SCENARIOS');ylabel('LOLE(/Yr)');grid on;  
set(gca,'XTick',1:6,'XTickLabel',name1g);  
  
figure,plot(1:6,EENS,'r-s','linewidth',2);  
xlabel('SCENARIOS');ylabel('EENS(kWh/Yr)');grid on;  
set(gca,'XTick',1:6,'XTickLabel',name1g);  
  
figure,plot(1:6,COST_OF_LOAD_LOSS,'r-s','linewidth',2);  
xlabel('SCENARIOS');ylabel('COST OF LOAD LOSS($/Yr)');grid on;  
set(gca,'XTick',1:6,'XTickLabel',name1g);
```

APPENDIX C: MATLAB code for the Economic Modelling

(Objective Process)

```

function
[fout, resfinal]=objective_process(datain, loadcurv, number_of_unit, for_val)

% Description      Replacement cost|Capital cost| Maintenance cost| FOR|
Lifetime
% Diesel generator 1521 $/kW          1521 $/kW          0.013 $/kWh       0.06
25000 hr
% PV                550 $/kW          550 $/kW          10 $/kW/yr        0.03
25 yr
% Battery           300 $/bat          300 $/bat          10 $/bat/yr        0.04  5
yr
% inverter           300 $/kW          300 $/kW          3 $/kW             0.03
15 yr

% ACS = (AMC+AFC+AEC+ACC+ARC)

% ACS Annualized cost of system ($/yr) RI Reliability index
% AEP Annual energy production (kWh/yr) EENS Expected energy not supplied
(kWh/yr)
% COE Cost of energy ($/kWh) loss C Value of lost load ($/kWh)
% AMC Annualized O&M cost ($/yr) AFC Annualized fuel cost ($/yr)
% AEC Annualized emission cost ($/yr) ACC Annualized capital cost ($/yr)
% ( ) i P C Probability of the state i ARC Annualized replacement cost
($/yr)
% AEC Annualized emission cost ($/yr)
% ACS= Annualized O&M cost + Annualized fuel cost + Annualized emission
cost + Annualized capital cost
% Annualized replacement cost
% ACS = (AMC+AFC+AEC+ACC+ARC);

mgpara=[1521 1521 0.013    0.06 25000/25000
         550  550  10      0.03 25
         300  300  10      0.04 5
         130  130  3       0.03 15
];
rlpcst=mgpara(:,1)./mgpara(:,5);
cpcst=mgpara(:,2);
if(number_of_unit==1)
    datain=[datain datain(3)];
    genunit=[datain];
    uint_power_generate=[rot90(cumsum(genunit(1)),2) 0];
else
    datain=[datain datain(3)];
    genunit=[datain];
    uint_power_generate=[rot90(cumsum(genunit(1)),2) 0];
end
%AMC=sum((datain).*( [0.013*25000 10/25 10/5 3/15] ))/100;
%AEC=sum((datain).*( [1200 0.2 0.3 0.4] ));
AFC=sum((datain).*( [ 0.07 0.0 0.0 0.0 ] ));
ARC=sum((datain).*(rlpcst. '))/100;
ACC=sum((datain).*(cpcst. '))/100;
ACS=(AFC+ACC+ARC);

```

```

for km=1:25
    mpcd(km)=ACS/((1+0.07).^km)*4;
end
NPC=round(sum(mpcd));
COE=ACS/540000;
prop_unavail=ones(1,number_of_unit).*for_val(1:number_of_unit);
prop_avail=1-prop_unavail;
indival_prop_system=prop_of_system(prop_avail,prop_unavail,number_of_unit);
for km=1:length(uint_power_generate)
    chk_lmt_exceed=find(loadcurv>uint_power_generate(km));
    totaltime=length(chk_lmt_exceed);
    final_lole(km)=indival_prop_system(km)*sum(loadcurv(chk_lmt_exceed)-
uint_power_generate(km));
    final_lolp(km)=totaltime*indival_prop_system(km);
    final_ens(km)=sum(loadcurv(chk_lmt_exceed)-uint_power_generate(km));
end
RI=sum(final_ens)*1.5;
fout=RI+ACS+COE;
resfinal=[round([AFC ACC ARC ACS NPC]) COE];

```

(Probability of the System)

```

function
indival_prop_system=prop_of_system(prop_avail,prop_unavail,number_of_unit)

ind=1;

indival_prop_system(ind)=prod(ones(1,number_of_unit).*prop_avail);
ind=ind+1;
for km=1:number_of_unit-1
    state_information=[zeros(1,km) ones(1,number_of_unit-km) ].';
    state_inf=state_information ;
    for kmx=1:number_of_unit-1
        prop_fail_info=circshift(state_information ,1);
        state_inf=[state_inf prop_fail_info];
        state_information=prop_fail_info;
    end
    system_up_and_down=state_inf;

system_up_and_down=sys_up_down_process(system_up_and_down,prop_avail,prop_u
navail);
    indival_prop_system(ind)=sum(prod(system_up_and_down));
    ind=ind+1;

end
indival_prop_system(ind)=prod(ones(1,number_of_unit).*prop_unavail);

```

(System UpDown Process)

```

function
finalres=sys_up_down_process(system_up_and_down,prop_avail,prop_unavail)
[rr,cc]=size(system_up_and_down);
for kc=1:cc
    sucess_fail_info=system_up_and_down(:,kc);
    locm1=find(sucess_fail_info==1);
    locm2=find(sucess_fail_info==0);
    sucess_fail_info(locm1)=prop_avail(locm1);

```

```
    sucess_fail_info(locm2)=prop_unavail(locm2);  
    system_up_and_down(:,kc)=sucess_fail_info.';  
end  
finalres=system_up_and_down;
```